

論文 / 著書情報
Article / Book Information

Title	Experimental investigations on suffusion characteristics and its mechanical consequences on saturated cohesionless soil
Authors	Lin Ke, Akihiro Takahashi
Citation	Soils and Foundations, Vol. 54, Issue 4, pp. 713-730
Pub. date	2014, 8
DOI	http://dx.doi.org/10.1016/j.sandf.2014.06.024
Creative Commons	See next page.
Note	This file is author (final) version.

License



Creative Commons: CC BY-NC-ND

**Experimental investigations on suffusion characteristics and its mechanical
consequences on saturated cohesionless soil**

Lin Ke and Akihiro Takahashi*

Lin Ke
Graduate student, Department of Civil Engineering,
Tokyo Institute of Technology, Japan
E-mail: ke.l.aa@m.titech.ac.jp

Akihiro Takahashi*
Associate Professor, Department of Civil Engineering
Tokyo Institute of Technology, Japan
E-mail: takihiro@cv.titech.ac.jp
* Corresponding author

Soils and Foundations, 54(4), 713-730, 2014

Original URL:

<http://dx.doi.org/10.1016/j.sandf.2014.06.024>

Abstract

The characteristics of suffusion and its mechanical consequences on saturated cohesionless soil with different initial fines contents at various stress states are presented in this paper. A series of seepage tests is performed by constant-flow-rate control mode with the measurement of the induced pore water pressure difference between the top and bottom of the tested specimen under the isotropic confining pressure. Back pressure is maintained constant in the tested soil specimen to ensure fully saturated soil condition. Cumulative eroded soil mass is continuously recorded by a consecutive monitoring system. Suffusion induced axial strain and radial strain of the 70mm-in-diameter and 150mm-in-height specimen is recorded during the seepage tests. The gap-graded cohesionless soil, which are assessed as internally unstable by existing evaluation methods, are tested. The mechanism of suffusion is demonstrated by the variation of hydraulic gradient, hydraulic conductivity, percentage of cumulative fines loss and volumetric strain during suffusion. The parametric study on the influence of two variables, effective stress level and initial fines content, on the mechanism of suffusion is elaborated. The mechanical consequences of suffusion are evaluated by conducting monotonic drained compression tests on the eroded specimens. Companion specimens without suffusion are tested for comparison purpose. The test results reveal that with the progress of suffusion, hydraulic gradient would drop and hydraulic conductivity would increase. Large amounts of fines are eroded away and correspondingly, contractive volumetric strain occurs. The larger effective confining pressure would lead to the less extent of suffusion. With larger initial fines content, more fines would be eroded away. The monotonic compression tests indicate that suffusion would cause the reduction of the soil strength at the major stage of drained shearing.

Keyword: suffusion, gap-graded cohesionless soil, triaxial test, saturated, deviator stress

1 Introduction

Significant damage to the high embankments of mountainside roads was observed during Noto Peninsula Earthquake of Japan in 2007: the road facilities in approximate 80 places have been damaged (Sugita *et al.*, 2008). A number of the damage was the flow slide of embankments constructed on catchment topography such as swamps and valleys which is usually accompanied with a large volume of fresh water. It is possible that those earth structures have suffered from years of erosion, which chronically turned the soil packing becoming loose, and consequently was vulnerable to seismic shaking. Similarly, numerous soil structure failure reported in literature was attributed to soil erosion. Crosta and Prisco (1999) presented a slope failure along an old fluvial terrace in Italy. By site investigation and numerical analysis, the authors concluded that seepage erosion and tunnel scouring in the superficial layers, and seepage erosion at the slop toe would be the vital factors triggering the failure. Muir Wood (2007) reported two large sinkholes, formed by internal erosion, were observed at the crest of the W.A.C Bennett Dam in Canada, which would be huge threats to dam safety. Richards and Reddy (2007) concluded that approximately half of the world's dam failure was related to soil erosion. Mainly, the soil erosion could be triggered by piping of soil grains through concentrated leak, backward erosion, suffusion or dispersion. To clearly recognize the seepage-induced internal instability of soil, the clarity of each term by definition is necessary: (1) piping refers to the phenomenon that underground water flows along continuous openings such as cracks and the soil on the wall of the tubular “pipe” is progressively washed away with the seepage flow, forming several large and instable soil channels which would produce

significant loss of soil integrity; (2) backward erosion indicates the erosion of soil grains at the exit of a seepage path such as the downstream face of a homogeneous embankment where the erosion resistance of the soil is highly dependent on the hydraulic gradient and the soil stress state; (3) suffusion describes the phenomenon that fine soil grains are eroded through the voids between the coarse grains by seepage flow, usually accompanying with amounts of seepage flow over the years; (4) dispersion results from chemically induced erosion of clay soils which is mostly observed in rainfall erosion. Recent studies revealed that the initiation and progression phases of piping and soil internal erosion may be classified into four mechanisms: i) suffusion, ii) contact erosion, iii) backward erosion, iv) concentrated leak erosion ([Fry, 2012](#); [Fell and Fry, 2013](#)).

This paper focuses on the characteristics of suffusion. At the beginning of 20 century, Russian researchers have published a comprehensive study about the phenomenon of the selective erosion of fine grains through a coarse matrix ([Goldin and Rumyantsev, 2009](#)). The fine grains are transported through the voids between the larger grains by seepage flow. Now this phenomenon is named as “suffusion” in hydrology or “percolation” in the power industry. It develops chronically with quantities of seepage flow over a period of years. [Kovacs \(1981\)](#) divided the suffusion into two subcategories: Internal suffusion and external suffusion. “Internal suffusion” occurs when the hydrodynamic forces are large enough to move fine grains from soils, affecting the local hydraulic conductivity. In contrast, the “external suffusion” occurs at the surface of a soil layer, which is “when the volume of the solid matrix is reduced, accompanied by an increase in permeability, but the stability of the skeleton composed of the coarse grains is unaffected”. Recently,

refinement of the definition is presented. [Moffat and Fannin \(2006\)](#) separated the phenomenon as “suffusion” and “suffosion”. They noted that “Internal instability describes the migration of a portion of the finer fraction of a soil through its coarser fraction. Redistribution of the finer fraction, termed suffusion, may yield a loss of grain and instigate a process of undermining, termed suffosion.” [Richards and Reddy \(2007\)](#) clearly defined suffusion as “the phenomenon that the finer fraction of an internally unstable soil moves within the coarser fraction without any loss of matrix integrity or change in total volume”, whereas suffosion, “on the other hand, means the erosion of grains would yields a reduction in total volume and a consequent potential for collapse of the soil matrix”. In this paper, the widely accepted term “suffusion” is used.

Soils vulnerable to suffusion are often thought of internally unstable, indicating that the constrictions formed by coarser fractions which constitute the soil skeleton are sufficiently large to allow the free passing of fines. A variety of empirical methods have been proposed to assess the instability potential for a soil ([US Army Corps of Engineer, 1953](#); [Istomina, 1957 \[Ref. Kovacs \(1981\)\]](#); [Kezdi, 1979](#); [Kenney and Lau, 1985, 1986](#); [Burenkova, 1993](#) and [Mao, 2005](#); [Chang and Zhang, 2013](#); among others). Those investigations introduce the “filter” concept whereby coarser fractions serve as a filter if water flows through. Whether or not the finer fractions would be potentially flushed off depends on the effective grain size ratio between the filter and fines. The ratio should not exceed an empirically derived threshold. The frequently used representative grain sizes are D'_{15} , D'_{85} of the coarse fraction, and d'_{15} , d'_{85} of the fines fraction in a soil. The effective grain size ratio virtually represents the slope of a gradation curve which

highlights the variation in grain size over a designated interval of the curve. [Chapuis \(1992\)](#) analyzed several empirically derived methods for internal stability assessment of granular soils and unified the criteria to one parameter which is the slope of grading curve. Different methods propose different curve slope values. On the other hand, from the perspective of micromechanics, the effective grain size of coarse fractions acclaimed in those methods may represent the constriction size in soil. [Terzaghi and Peck \(1948\)](#) proposed $D_{15}/4$ to quantify the constriction size in filter and then the soil retention criterion $D_{15}/4 < d_{85}$ is derived. Similarly, [Kezdi \(1979\)](#) noted the value of $D'_{15}/4 \sim D'_{15}/5$ can approximate the constriction size in the coarse fraction by assuming a contacting spheres packing of soil. [Kenney and Lau \(1985\)](#) inferred the predominant constriction size in the voids of a filter is approximately equal to the grain size of the soil making up the filter for which 25% by weight is finer. Thanks to the advances in computer science, theoretical assessment of constriction size could be approached in detail. [Reboul et al. \(2010\)](#) and [Vincens et al. \(2012\)](#) summarized the method of evaluating the constriction size distributions of a numerical assembly of spheres which were generated by Discrete Element Method (DEM). The measurement of the void geometry was fulfilled by a radical Delaunay tessellation. Since high computational expense is necessary for such evaluation, a simple probabilistic based alternative is commonly used. [Silveira \(1965\)](#) assessed the soil filtration/retention by analyzing cumulative constriction size distribution (CSD) which was derived from grain size distribution with assumptions of geometric packing. He examined the probability of a soil grain with equivalent size passing through a probable path in a granular medium, which depends on the constriction sizes of the voids and their occurrences within the filter. [Locke et al. \(2001\)](#) and [Indraratna et al.](#)

(2007) adopted the developed CSD to solve the time-dependent filtration related issues and improve the retention criterion for nonuniform granular filter design, respectively. A detailed summary of the abovementioned criteria for suffusion assessment could refer to [Marot and Benamar \(2012\)](#).

The initiation of suffusion on potentially unstable soil would be triggered if the hydrodynamic forces induced by the seepage flow on soil grains exceed a critical threshold. In laboratory investigations, the seepage flow is maintained by assigning a hydraulic pressure difference or a constant water flow. The critical threshold, termed “critical hydraulic gradient” or “critical flow rate”, represents the onset of suffusion ([Moffat *et al.*, 2011](#); [Richards and Reddy, 2012](#)). Due to the complexity in soil packing, stress state and controlled hydraulic condition, a widely accepted method to determine the critical value may not exist. The adaptability of the recorded data in literature to other regions depends on the similarity of the fluid/soil condition with that in laboratory tests. Here the significance of stress state should be stressed. As is universally recognized, the behavior of soil is highly influenced by its stress state. However, hitherto, the effect of stress state on erosion mechanism is obscure and controversial. [Tomlinson and Vaid \(2000\)](#) concluded that the larger confining pressure may trigger erosion in artificial granular materials at a smaller gradient because of the disturbance of soil arching. This tendency is especially obvious for the soil specimen with small grain size ratio (D'_{15}/d'_{85}). [Wan and Fell \(2004\)](#) noted that the degree of compaction had a minor effect on the erosion rate of silty and cohesive natural soils comparing to the water content and corresponding degree of saturation. [Bendahmane *et al.* \(2008\)](#) showed that for

cohesiveless soil, the erosion rate tends to increase with the rising of confining pressure. They assumed the existence of a secondary critical gradient. If the assigned hydraulic gradient is below this value, the confining pressure tends to increase the soil resistance to suffusion, whereas the assigned hydraulic gradient is larger than this value, backward erosion begins. [Chang and Zhang \(2012\)](#) conducted suffusion tests at isotropic stress state, compression stress state and extension stress state. They divided the erosion process into four phases corresponding to the characteristic hydraulic gradient in each. The maximum eroded soil mass was detected at the extension stress state.

For the non-cohesive soils, due to the large amounts of loss in fines, suffusion may render a loose soil structure with increased porosity and hydraulic conductivity. The strength of the post-suffusion soil may decrease due to the destructive function of suffusion. Few studies could deliver comprehensive investigations about the consequences of suffusion from the perspective of soil mechanics. [Muir Wood *et al.* \(2010\)](#) modelled the mechanical consequences of suffusion by two-dimensional discrete element analysis. In their approach, the progress of suffusion was approximated by progressively removing grains from assemblies of circular discs at different stages of shearing. The simulation indicated that suffusion may trigger the soil state changing from “dense” (below the critical state line) to “loose” (above the critical state line). Similarly, [Scholtès *et al.* \(2010\)](#) noticed that the soil behavior altered from being dilative to contractive when extracting the fine grains. Those zones in the earthen structure where suffusion occurs would be more prone to fail. [Xiao and Shwiyhat \(2012\)](#) conducted undrained compression test on post-suffusion soils and found that the peak deviator stress of

suffusional soil was larger than the soil without suffusion, which may be attributed to the low degree of saturation. [Hicher \(2013\)](#) modelled the effects of particle removal on the behavior of granular materials and concluded that removal of soil particles may cause diffuse failure in eroded soil mass.

A comprehensive understanding of the suffusion mechanisms and the post-suffusion soil behavior is beneficial to the estimation of suffusion progress and is helpful for the retrofit of internally eroded soil structures, such as levees. The main purpose of this study is to experimentally investigate the characteristics of suffusion and its mechanical influence on saturated gap-graded cohesionless soil under the isotropic confining pressure using a newly developed triaxial permeameter which is capable of maintaining back pressure in the soil specimen during suffusion test and directly measuring the cumulative eroded soil mass within the test period. The suffusion-induced variation of soil hydraulic conductivity, volumetric strain and void ratio is presented. Mechanical consequences of suffusion are revealed by conducting drained monotonic test on the suffusional specimens and comparing the outcoming results with the mechanical responses of the companion specimens without suffusion.

2 Experimental investigations

2.1 Triaxial permeameter

The newly developed triaxial cell mainly consists of a constant-flow-rate control unit, an

automated triaxial system and eroded soil collection unit. Schematic illustration of the overall system is shown in Fig. 1 (Ke and Takahashi, 2014). The cell accommodates a specimen of 0.07m-in-diameter and 0.15m-in-length. The constant-flow-rate control unit is mainly composed of a rotary pump with the maximum flow rate of $2.27 \times 10^{-5} \text{m}^3/\text{s}$ for controlling water flow downwardly through the specimen and a Low Capacity Differential Pressure Transducer (LCDPT) for measuring the pressure drop within the tested specimen. The output of LCDPT is highly linear within the range of 0~20kPa. Two pore pressure transducers are installed at the top and bottom of the specimen respectively to double check the pressure difference. The size of flow tubes is designated as 0.0075m-in-diameter. During the experiment, the range of assigned inflow rate must ensure the resulting pressure drop is well below the confining pressure to prevent the separation of membrane from the specimen. A perforated plate with several 0.001m openings is mounted in the top cap, which directly attaches specimen, to minimize the possible induced head loss. Another plate is at the base pedestal serving as a filter (Fig.1). It is a 0.005m-thick and 0.07m-in-diameter circular steel mesh with a smooth surface. The opening size of the filter is determined as 0.001m following the specifications of the Japan Dam Conference (Uno, 2009) that the mesh should fully hold the coarse fractions of an unstable soil and allow the passing of fine fractions. A plastic tube is fitted at the outlet of the trough, directly connected to the soil collection system. Downward seepage flow is selected for testing due to the feasibility of triaxial permeameter. It is possible to revise the pedestal to provide sufficient drainage space and conveniently collect eroded fines. In literature, several suffusion tests were conducted by upward seepage flow (Sterpi, 2003). Richards and Reddy (2012) concluded that the seepage direction significantly

altered the critical velocity. A larger value of critical velocity was detected for the tests conducted at the angles between gravitational force and the seepage vector above the horizontal.

The automated triaxial system used could conduct measurements and controls by PC through 16-bit A/D and D/A converters. The vertical load could be automatically applied by a motor-gear system at any rate. The maximum load is 50kN. The cell pressure is applied by air pressure which is maintained constantly at 700kPa through an automatic air compressor regulated by E/P (Electronic to Pneumatic) transducers. All the pressure lines are connected to a draining system to remove any condensed water. The deviator load is measured by a submersible load cell mounted inside of the cell. The effective pressure is measured by the differential pressure transducer connected between the specimen base and cell. Back pressure is applied from the bottom of the specimen via a 10^{-4}m^3 volume gauge during consolidation test. Axial displacement is measured externally by a Linear Variable Differential Transformer (LVDT). Three pairs of clip gauges with the maximum capacity of $\pm 0.002\text{m}$ are employed to measure the radial strain.

The eroded soil collection unit is the pressured sedimentation tank that consists of the acrylic tube mounted between a steel top and base plate, and sealed by means of O-rings and five external tie rods. A light tray for collecting the eroded soil grains is submerged in a 0.16m-in-diameter acrylic cylinder and hooked to the load cell that is attached to a steel frame. A funnel, with a 0.015m-in-diameter opening at the end is fastened surrounding the inlet pipe to minimize the flow jet effect. The waterproofed load cell has high

sensitivity that could record the mass of eroded soil within the test period. A solenoid valve with a timer is fixed on the outlet drainage line to drain the seepage water away at a determined interval of time. During suffusion tests, the back pressure is applied to the tested specimen from this sedimentation tank.

2.2 Test materials

Gap-graded soils, like sandy gravels, are more prone to suffusion due to its deficiency in certain grain size (Skempton and Brogan, 1994). They may be detected at the earth dams that have been suffered from years of suffusion or the construction site with substandard procedure of soil mixing leading to the omission of amounts of soil grains. In this study, the gap-graded soils consist of the binary mixtures of silica sands (silica No.3 and No.8, shown in Fig. 2) with different dominant grain sizes. The silica sand is mainly composed of quartz, categorized as sub-round to sub-angular material. According to the Unified Soil Classification System (ASTM D2487), they correspond to SP. The grain size distributions are shown in Fig. 3. In the mixtures, silica No.3 with larger grain size serves as the coarse fraction while the fine silica No.8 is the erodible fines within the voids between the coarse grains. Ke and Takahashi (2012) estimated the maximum mass fraction of fines is approximately 37% for the tested mixtures derived from the geometrical restriction: the volume of fines should be less than that of the voids between coarse grains. A series of fines content (mass ratio of fines to total weight of soil specimen) of 35%, 25% and 15% is adopted. It is worth stressing that maximum mass fraction of fines is derived based on an ideal condition that coarse grains are loosely packed and fines are densely packed

between coarse grains. In reality, it is difficult to reach such ideal condition. Therefore the maximum mass fraction should be less than 37% depending on the soil fabric and geometry properties of soil grain. The grain size distribution and the physical properties of the mixture are shown in [Fig. 4](#) and [Table 1](#). The vulnerability of the mixture to suffusion is assessed by currently available methods. The details of the evaluation are shown in [Table 2](#), which indicates that the mixtures are potentially unstable for suffusion.

Several internally unstable specimens are tested to understand the suffusion mechanism. A summary of the test cases is shown in [Table 3](#). Each specimen with moisture content is tamped to the target void ratio. The applied mean effective stress is 50kPa, 100kPa and 200kPa, which approximately corresponds to the earth pressure of 5m, 10m and 20m in depth, respectively. Monotonic drained compression is conducted on the suffusional specimens to understand the mechanical consequences of suffusion. Controlled specimens (35N-50, 25N-50 and 15N-50) at the same stress state without suffusion are tested for the comparison purpose. Three specimens, named 35E-50-R, 35E-100-R and 35E-200-R, are tested at the same effective stress state as that of specimens 35E-50, 35E-100 and 35E-200 to confirm the repeatability of the test results and the apparatus.

3 Test procedures

The moist tamping method ([Ladd, 1978](#)) is employed to prepare a specimen for minimizing the segregation of the two different sized grains. The specimen is compacted to the target void ratio by 10 layers and the height of each layer is determined by

“undercompaction” at the initial moisture content of 10%. From previous trials and errors, a uniform specimen would be achieved at this moisture content. The wet soil is kept in a zipped bag to equalize moisture at least 16 hours before use. Since the soil weight could not be directly measured after preparation, the after-test oven-dry weight of the specimen together with the eroded soil weight should be checked. The reconstituted specimen is 0.07m in diameter and 0.15m in height.

The vacuum saturation procedure ([JGS 0525-2000](#); [ASTM D4767-11](#)) is adopted in this study. Upon the completion of specimen preparation, the top and the bottom of the tested specimen is connected to a lower and an upper reservoir, respectively. Both of the reservoirs are 0.1m in diameter and 0.3m in height. Vacuum is supplied to the specimen through both water reservoirs gradually until -80kPa, keeping the pressure difference inside and outside the specimen constant. Allow deaerated water in the upper reservoir slowly inject into the specimen from the bottom. Considering that the tested specimen is internally unstable, the inflow rate should be sufficiently slow to avoid soil grain migration in the specimen (i.e., $5.56 \times 10^{-9} \text{m}^3/\text{s}$). After three-quarters of the deaerated water in the upper reservoir has flowed through the specimen, slowly reduce the vacuum in the specimen to 0kPa and increase the cell pressure to 20kPa, keeping the pressure difference constant all the way. Then let the deaerated water inject into the specimen again. The deaerated water with a total volume of 10.4 (normalized value in terms of pore volume) has been flowed through the soil specimen before suffusion test. The inlet valve of the sedimentation tank should be closed all the way to avoid any possible soil loss. For the majority of tests, B values of at least 0.95 could be achieved after applying back

pressure of 100kPa following the vacuum saturation procedure.

The consolidation is performed by an automatic control system. Cell pressure gradually increases up to the target value at a fairly small increment (i.e., 1kPa/min) to avoid the migration of soil grains. Axial stress, controlled by a motor, increases correspondingly to keep the determined effective stress ratio (effective axial stress/effective radial stress) constant. In this study, soil specimens are isotropically consolidated until the preferred stress state is reached.

The stress state during the suffusion test is maintained the same as that of the isotropic consolidation. The axial displacement, radial deformation, the pore water pressure difference generated by the seepage flow and cumulative eroded fine mass is recorded at every 1s automatically. To logically demonstrate the mechanical effects of suffusion on soils, the imposed inflow rate for each specimen is held constant. After several trial tests, an inflow rate of $5.17 \times 10^{-6} \text{ m}^3/\text{s}$ is selected due to the relatively large fines loss at this rate. The procedure of inflow rate increments in this study is shown in Fig. 5. The initial increment of inflow rate is set approximately at $1.67 \times 10^{-7} \text{ m}^3/\text{s}$ per min: increase the inflow rate to $1.67 \times 10^{-7} \text{ m}^3/\text{s}$ in 1min and allow the seepage flow to become steady for the next 1min. The initiation of suffusion approximately occurs within the inflow rate of $5.00 \times 10^{-7} \sim 1.00 \times 10^{-6} \text{ m}^3/\text{s}$. As long as suffusion initiates, the amounts of eroded fine grains would increase with the increasing of inflow rate. The increments at this stage could be relatively larger to shorten the test. In this study, the inflow rate is increased to the target value at the incremental rate of $8.33 \times 10^{-7} \text{ m}^3/\text{s}$ per min. The inflow rate is

maintained constant until (1) the recorded hydraulic gradient is steady; (2) the effluence become clear and clean by visual observation; (3) no further eroded fines loss (i.e., <0.2g per 600s); (4) no further increases in the volumetric strain of the tested specimens. The suffusion tests would be terminated at least after 3 hours. In most circumstances, the post suffusion B-value is larger than 0.93. During suffusion test, since the pore pressure at bottom is maintained constantly at 100kPa, the downward seepage flow may increase the pore pressure at the top of a tested specimen and consequently, reduce the effective stress linearly along the specimen. The specimen may be unloaded during suffusion test and a mild recovery of volumetric strain is expected. However, the test results indicate a quite limited influence of the distribution of effective stress along the specimen on the volumetric strain and the hydromechanical behavior of tested soil is considered to be mainly governed by filtration law within the scope of this study.

After the suffusion test, drained compression test is performed at the same stress state as that of suffusion test to investigate the mechanical consequences of suffusion. The compression test is displacement controlled with an axial strain rate of 0.1%/min, following the standard criteria ([JGS 0524-2000](#); [ASTM D7181-11](#)), to allow the pore pressure to reach equilibrium. The confining pressure is maintained constant while axial displacement increases at the designated strain rate. Axial stress could be obtained from the load cell amounted to the piston. The recorded data from the eroded soil collection unit indicate that there is hardly fines loss due to compression.

4 Test results

Parametric study is performed in this series of tests. Two variables in this study are the effective confining pressure (50kPa, 100kPa and 200kPa) and initial fines content (35%, 25% and 15%), which are considered of great significance for suffusion phenomena. Firstly, the characteristics of suffusion are described by interpreting the hydraulic gradient, cumulative eroded soil mass and volumetric deformation of the tested specimens with 35% initial fines content under the effective confining pressure of 50kPa (specimen 35E-50). One of the consequences of suffusion is the variation in grain size distribution curve, which would be helpful to illustrate the spatial progression of suffusion. Then, the influence of the two variables is discussed by the comparison of the testing data of other specimens with those of specimen 35E-50.

4.1 Saturation degree

The saturation degree of the tested specimen would usually decrease during the period of the suffusion test because of the air bubbles generated in the specimen induced by the pore pressure reduction. Commonly, the inflow is at the larger pressure with air dissolved. Due to the head loss during suffusion test, the pore water pressure in the tested specimens is lower. Thus, dissolved air may probably separate out and form air bubbles in the tested specimen. As a result, the saturation degree would decrease. [Evans and Fang \(1988\)](#) proved that the decrease in saturation degree would cause the reduction in the measured hydraulic conductivity by approximately three orders of magnitude, which may result in a misleading understanding of the hydraulic behavior of tested sand. Furthermore, falling

in the saturation degree may reduce the quality of compression test on the suffusional specimens. As a countermeasure, a back pressure of 100kPa is applied to the tested specimens from the sedimentation tank, shown in Fig. 6. Although slight deviations from 100kPa exist due to the regular opening/closing of drainage valve of sedimentation tank, basically the back pressure is maintained constant in the tested soil specimen. Usually, the B-value drops after suffusion test. For most of the soil specimens, that value is still larger than 0.93, which is considered as fully saturated in this paper.

4.2 Change of hydraulic gradient and conductivity with time

The hydraulic gradient is derived from the recorded pressure drop induced by seepage flow and the specimen length corrected by deducting the vertical deformation. With the progress of suffusion, hydraulic gradient would vary correspondingly. That variation of specimen 35E-50 at the initial 900s and 0s~11000s in the suffusion test is plotted in Fig. 7. At 480s, a moderate drop of hydraulic gradient is noticed (inflow rate $Q=8.33\times 10^{-7}\text{m}^3/\text{s}$, Darcy velocity $v=2.1\times 10^{-4}\text{m/s}$), which is considered as the sign of the onset of suffusion (Fig. 7a). The effluent becomes slightly turbid with very small amounts of suspending fines. At this moment, the reading from the eroded soil collection unit is basically zero, indicating that no eroded fines are detected. It is postulated that at this stage the process of filtration of fine grains diffuses within the specimens. A sharp increase of the hydraulic gradient is detected at 880s ($Q=1.67\times 10^{-6}\text{m}^3/\text{s}$, $v=4.2\times 10^{-4}\text{m/s}$) at which the increment of the inflow rate begins increasing from $1.67\times 10^{-7}\text{m}^3/\text{s}$ per min to $8.33\times 10^{-7}\text{m}^3/\text{s}$ per min (Fig. 7b). This sharp increase may relate to the influence of “hammer effects” which

refers to the phenomenon that a sudden increase or decrease in Darcy velocity would affect the hydraulic properties of soil specimens (Tomlinson and Vaid, 2000). It may induce the unexpected movement of soil grains that may cause temporary clogging. The hydraulic gradient dramatically drops after the “peak” with the erosion of a large amount of fines. It is postulated that the soil grains gradually change their position for self-balance at this stage and correspondingly, the specimen would deform. After a certain period, the packing of soil grains will reach a new equilibrium without further erosion of fines. As a result, the hydraulic gradient becomes constant.

On condition that Darcy velocity and hydraulic gradient is known, hydraulic conductivity could be calculated following Darcy’s law that describes the flow of a fluid through a porous medium. In this study, the inflow is constantly provided by a pump with a constant rate. Discharge rate is unknown due to the difficulties in conducting measurement in a pressurized tank. The Darcy velocity in this assessment is derived from the inflow rate and the cross-sectional area corrected by the radial deformation. Figure 8 shows the variation of hydraulic conductivity with the period of suffusion test. Before the onset of suffusion, hydraulic conductivity keeps constant at $6.0 \times 10^{-5} \text{m/s}$. At the initial drop of hydraulic gradient, hydraulic conductivity begins increasing at 480s ($Q=8.33 \times 10^{-7} \text{m}^3/\text{s}$, $v=2.1 \times 10^{-4} \text{m/s}$, Fig. 8a). An obvious increase of hydraulic conductivity is observed after the sharp increase of hydraulic gradient (Fig. 8b). It could be understood that with the progress of suffusion, the fines are gradually dislodged causing the increasing of pore size. Thus, hydraulic conductivity increases. It may be argued that the temporary clogging, which leads to the sharp increase of hydraulic gradient, should decrease the

hydraulic conductivity. In this study, the formation and dissipation of the temporary clogging is found to be rapid in a short period probably because of the relatively large hydraulic conductivity of the tested soil. Therefore, a mere increasing of hydraulic conductivity is obviously noted in Fig. 8b. Seepage flow would carry a significant amount of fines through the channels formed by voids among coarse grains. It is possible that the movement of fines is impeded at a channel, the size of which is not sufficiently large for passing of fines and consequently, it may result in clogging. With the increasing accumulation of fines at channels, the size of effective pore throats would further decrease and thus, hydraulic conductivity would drop. This phenomenon is usually detected after a significantly longer period. In this study, the decrease of hydraulic conductivity from 8500s probably indicates the possible occurrence of clogging. The maximum hydraulic conductivity detected is approximately 150 times larger than the initial value.

4.3 Cumulative eroded soil mass with time

The evolution of the percentage of cumulative fines loss with time is plotted in Fig. 9 where the recorded cumulative eroded soil mass is normalized by the total weight of specimen before suffusion. Corresponding to the instantaneous increase of hydraulic gradient, large amounts of fines are eroded away, which might cause the increment of porosity and the re-adjustment of the inter-grain position. The erosion rate decreases with the progress of suffusion. By the end of the test ($t=11000s$, $Q=5.17\times 10^{-6}m^3/s$, $v=1.4\times 10^{-3}m/s$), approximately 25% fines are lost and 13% fines remain in the tested specimen.

4.4 Volumetric deformation with time

The incessant erosion of fines from the tested specimen may result in the re-arrangement of soil grains, consequently leading to the volumetric deformation. [Figure 10](#) presents the soil specimen deformation in terms of volumetric strain during the suffusion test. At the stage 1 of the suffusion test when the inflow rate increases from 0 until $1.67 \times 10^{-6} \text{m}^3/\text{s}$ by $1.67 \times 10^{-7} \text{m}^3/\text{s}$ per min, the volumetric strain approximately increases by 2.3% because of the test apparatus. The rotary pump used in the test would produce jet flow on the soil specimen when increasing the inflow rate, i.e., at the beginning of each stage. This jet flow leads to the soil deformation, which is considered as a limitation of the current water circulation system of the permeameter. Generally, the tested specimen is prone to be contractive with the progress of suffusion. In stage 3 when the inflow rate is kept constant, two obvious jumps in deformation are detected around 2400s and 5600s. It is postulated that along with the constant loss of fines, the coarse grains would correspondingly re-arrange their positions to reach a new equilibrium in a short period, which might be an explanation of the sudden and rapid collapse of earthen structure induced by suffusion. [Moffat et al. \(2011\)](#) described the relatively rapid volumetric deformation of soil as the characteristic of suffusion.

4.5 Post-suffusion grain size distribution

The variation in grain size distribution could reflect the changes in the geometry of soil

specimens due to suffusion. [Kenney and Lau \(1985\)](#) concluded that fine grain losses resulting from suffusion could cause the post-suffusion distribution curve shifts downward from original curve. The extent of the movement proportionally increases with the amount of fine grain loss. [Chang and Zhang \(2011\)](#) experimentally demonstrated that comparing to the fines loss in the bottom layer and the middle layer, that loss in the upper layer is larger. In this test, the post-suffusion specimen is equally divided into two layers: top layer and bottom layer. The grain size distribution curve is determined by sieving test on those soils that have been oven-dried at 110°C for 24h. [Figure 11](#) presents the typical grain size distributions of a post-suffusion soil specimen. The post-suffusion curves of both upper layer and bottom layer move downward from the original curve, the extent of which is corresponding to the loss of fines. Moreover, the fines loss in the upper layer is more than that in the bottom layer.

4.6 Influence of effective stress level

Hitherto, it is too complicated to fully understand the effects of stress level on suffusion. At the larger confining pressure, the fines are expected to be densely packed among coarse grains and the interstitial spaces may be narrower. For the soil specimens with the larger confining pressure, the seepage flow might dislodge fewer fines. However, the force transfer mechanism of granular material is much more complex. Due to the boundary frictions, force-arching may develop at the intersections of the bottom boundary, which may hold the fines from erosion. At the larger confining pressure, it is possible that the force-arching is failed, which, instead, might cause further erosion of fines. In this

study, constant-flow-rate suffusion tests on the specimens with 35% initial fines content under three different effective confining pressures (50kPa, 100kPa and 200kPa) are conducted. Through the period of suffusion test, the mean effective stress is kept the same as that of consolidation (e.g., $p'=50\text{kPa}$, $q=0\text{kPa}$). The influence of effective confining pressure is demonstrated by comparing the test data in terms of Darcy velocity, hydraulic conductivity, percentage of cumulative fines loss and volumetric strain.

The Darcy velocity for stage 3 under different effective confining pressures is presented in [Table 4](#). It indicates that the velocity is basically the same in each case, which provides a reference for the following comparison. [Figure 12](#) shows the normalized hydraulic conductivity, which is the ratio of the hydraulic conductivity after and before suffusion. For specimen 35E-50 whose effective confining pressure is 50kPa, the post-suffusion hydraulic conductivity increases nearly 150 times, whereas that increment for specimen 35E-100 and 35E-200 is 100 and 80, respectively. With the progress of suffusion, the specimen would gradually become heterogeneous and consequently, the local velocity field exhibits significant spatial fluctuations. It is possible that the local flow velocity is different from the overall macroscopic velocity. Under larger effective confining pressure, the maximum value of the local velocity field is lower and therefore, the progress of suffusion may slow down. On the other hand, the fines might be tightly packed and the interlocking between soil grains is firmer under larger effective confining pressure. Thus, fewer fines would overcome the interlocking forces and would be dislodged from the specimen, as is shown in [Fig. 13](#). As is discussed, the extent of the increasing in the hydraulic conductivity is closely associated with the amounts of fines loss. For the

specimen with less extent of increasing in hydraulic conductivity (i.e., specimen 35E-200), the fines loss is expected to be less (Fig.13). Similarly, the volumetric strain induced by erosion of fines is the least in specimen 35E-200 and the largest in specimen 35E-50, shown in Fig. 13.

4.7 Influence of initial fines content

The initial fines content actually characterizes the effect of soil packing, which may offer a physical explanation for the soil hydromechanical behavior. The schematic microstructure of the soil specimen with respective 35%, 25% and 15% fines content is shown in Fig. 14. Majority of fines is considered to be locked within the voids of coarse grains for the specimen 15E-50 with 15% initial fines content, in contrast with the specimen 35E-50 with 35% initial fines content, where the fines may not only fill the voids but also probably separate the coarse grains. If suffusion initiates, the fines simply occupied the voids may be easily eroded away while those fines separating the coarse grains may hardly move because of the larger contact force on them. Suppose that the fines are merely considered as voids, at the same relative density, the voids size among the coarse grains of specimen 35E-50 would be larger than that of specimen 15E-50. A larger void size would commonly allow for greater fines loss. Therefore, the specimen with larger initial fines content is assumed to show much greater extent of suffusion.

The Darcy velocity assigned on the specimens with different initial fines contents under an effective confining pressure of 50kPa is noted in Table 4. The similar value of flow

velocity for each specimen is regarded as a reference for comparison. The initial relative density of each specimen is set the same as 30%. The normalized hydraulic conductivity versus initial fines content is presented in Fig. 15, indicating that the largest increase of hydraulic conductivity occurs in specimen 35E-50. Figure 16 shows the percentage of cumulative fines loss and suffusion-induced volumetric strain versus initial fines content. It can be seen that cumulative fines loss is larger for specimen 35E-50 and correspondingly, the suffusion-induced volumetric strain is larger.

4.8 Test repeatability

The repeatability is confirmed by comparing the key parameters among tested specimens with 35% initial fines content, shown in Table 5. Irregular deviation exists among the hydraulic gradient and hydraulic conductivity, which might be influenced by the inhomogeneity of the specimens. However, the percentage of cumulative fines loss and volumetric strain are basically the same, which might indicate the consistency of erosion law for each test case.

5 Discussions

5.1 Evolution of void ratio

Change of void ratio is caused by the fines loss (ΔV_f) and possible intergranular rearrangement (ΔV), as is shown in Fig. 17. To address the problem, it is postulated that the

void ratio change follows two steps: (1) as soon as suffusion initiates, no deformation occurs due to the dislodgement of fines, the total volume of the tested specimen remains the same and the volume of eroded fines would be occupied by water at the same volume if the saturated soil is taken into consideration. e_c indicates the void ratio induced by erosion of fines without soil deformation, which can be given by:

$$e_c = \frac{e_0 + \Delta FC}{1 - \Delta FC} \quad (1)$$

Where ΔFC indicates the percentage of cumulative fines loss by mass, which equals to the percentage by volume if the specific gravities of the coarse and the fine grains are the same; (2) with the erosion of large amounts of fines, the metastable structure might be formed which would easily trigger the re-arrangement of soil grains into a stable packing. Correspondingly, a volumetric deformation (ε_v) and therefore a change in void ratio would take place, which equals to $\varepsilon_v(1 + e_c)$. The post-suffusion void ratio could be obtained as:

$$e = e_c - \varepsilon_v(1 + e_c) = (1 - \varepsilon_v) \left(\frac{e_0 + \Delta FC}{1 - \Delta FC} \right) - \varepsilon_v \quad (2)$$

As is indicated by Eq. (2), change of void ratio is closely dependent on the volumetric strain during suffusion. If no deformation occurs, a large post-suffusion void ratio would be obtained. Further, if the specimen shows dilative behavior during suffusion, the largest void ratio would be gained, which may again accelerate the suffusion progress. By contrast, a contraction behavior during this process may delay the increase of void ratio even decrease the void ratio after suffusion. At this circumstance, the lower limit of void ratio could be determined by the greatest density that the coarse grains could achieve. The

corresponding volumetric deformation of the specimen would reach the maximum value. [Scholtès *et al.* \(2010\)](#) conducted the simulations of grain extraction by the similar approach. The volumetric deformation (ε_v) of granular assembly was obtained by the analysis of inter-particle sliding resistance. [McDougall *et al.* \(2004, 2013\)](#) proposed a parameter, indicated by Λ , to quantitatively illustrate the dissolution-induced volume change of soil. It is defined as the ratio of the increments of void volume to that of solid volume. A value of -1 indicates no change in volumetric strain and the increase in void ratio is the maximum.

A plot of the amount of axial, radial and volumetric strain versus cumulative eroded fines loss is depicted in [Fig. 18](#) to interpret the deformation characteristics during suffusion. The positive axial, radial and volumetric strains indicate the contractive behavior of the tested specimen. Initially, the inflow rate is small and few fines are eroded away while the jet flow induced by the flow pump causes certain amounts of strain. From the beginning of stage 2, large amounts of fines are dislodged and soil deformation develops correspondingly. The phenomenon of the jumping of radial strain frequently occurs while the axial strain develops smoothly. [Chang and Zhang \(2012\)](#) proposed that the soil deformation is mostly determined by the potential of buckling of the strong force chains through the coarse grains and fine grains mainly provide lateral supports for those chains. Since the mass of coarse fractions keeps constant during suffusion, failure of a force chain may let the remaining force chains to keep on supporting the soil specimen and therefore, the axial strain smoothly develops. On the other hand, the fines loss is continuous with the progress of suffusion, which would continuously weaken the lateral

supports. At certain circumstances, when the remaining fine grains are not strong enough to provide the lateral support, sudden radial deformation may occur, which is represented as “jumps” in radial strain. Another potential possibility relates to the strain-measuring techniques employed in the triaxial testing. The axial strain is recorded by an external LVDT, directly connected to the loading piston and top cap. Since the top cap equally spaced around the top surface of the tested specimen, the measured axial strain actually represents the average displacement and therefore, the recorded curve develops smoothly. For the radial strain determination, on the other hand, it is obtained from three clip gauges attached at the different spots along the specimen. The inherent assumption is that the average of the discrete radial deformations is representative of the overall radial strain. Comparing to the whole body measurements of axial strain, the discrete local radial deformation might be discontinuous with possible abrupt irregularities.

The estimated void ratios derived from Eqn. (1) and (2) for the specimens with 35% initial fines content under an effective confining pressure of 50kPa are presented in **Fig. 19**, which clearly indicates the contribution of volumetric strain to the void ratio change. For specimen 35E-50, the calculated void ratio considering mere fines loss is 1.13 and because of the volumetric deformation that value approximately decreases by 3.5% to 1.09. The calculated value of Λ is -0.91 for the specimen, indicating a limited influence of volumetric strain on the increments of void ratio. At the larger confining pressure, with less loss in fines, the volumetric deformation of the tested specimen and void ratio change is comparatively less. Compared to the soil state before suffusion, the post-suffusion void ratios commonly increase, which might alter the mechanical response of

the tested soil in terms of stress-strain relationship.

5.2 Erosion law

The constitutive law for erosion is mostly empirical, derived from laboratory tests. For cohesive soil, [Reddi *et al.* \(2000\)](#) proposed an expression of shear stress to evaluate the initial surface erosion. Afterwards, a number of internal erosion analysis adopted this concept with the assumption that as long as the seepage flow exerted shear stress is larger than the critical shear stress, erosion occurs ([Fujisawa *et al.*, 2010](#)). However, if the size of the flow path within the specimen and that of the eroded fines are considered, there is high possibility of occurrence of soil redeposition and clogging. In this paper, the erosion by definition refers to the effective dislodgement and transport of the fines, which would be detected at the exit of the tested specimens. The test results are summarized in [Figs. 20 and 21](#) in terms of evolution of (a) percentage of cumulative fines loss with time and (b) erosion rate with hydraulic gradient under different effective confining pressures and initial fines contents. It is noted that both the cumulative eroded soil mass and maximum erosion rate decrease with the effective confining pressure and increase with the initial fines content within the test range. The erosion rate reaches the peak after the onset of suffusion and then drops to a constant value. This tendency is in accordance with the finding of [Reddi *et al.* \(2000\)](#), who conducted the laboratory test by a flow pump.

5.3 Mechanical consequences of suffusion

The deviator stress and volumetric strain are plotted versus the axial strain in [Figs.22 and 23](#) for the respective specimens without and with suffusion. The tested specimens contain 35%, 25% and 15% initial fines content under an effective confining pressure of 50kPa. The void ratio and fines content before compression are denoted in the figures. By comparing the drained response of the specimens without suffusion, the soil strength and stiffness show a larger value for the less initial fines content, but no much difference can be seen in the volume changes. The exceptional drained response is found in specimen 25N-50, which exhibits somehow similar deviator stress as that of specimen 35N-50 at the medium strain level and relatively large volumetric strain. It may be understood from the characteristics of the fines content dependent soil packing. Previous works noted the fines content dependent soil behavior: a threshold fines content, denoting the soil fabric transform between “sand-in-fines” and “fines-in-sand”, exists ([Vallejo, 2001](#); [Huang, et al., 2004](#); [Yang, et al., 2006](#); [Shipton and Coop, 2012](#); among others). The soil with the threshold fines content may exhibit the peculiar responses in the deviator stress and volumetric strain comparing to those with different fines contents. [Chang and Meidani \(2012\)](#) demonstrated that the fines content of 25% signifies that fines almost occupy the voids of coarse grains and begin separating the sand grains while that larger than 35% stands for the full isolation and floating of coarse grains in a network of fines. Correspondingly, it is inferred that in this study 25% fines content is the threshold value by which specimen 25N-50 appears to behave exceptionally. In terms of the drained response of the specimens with suffusion, since the post-suffusion fines content is approximately similar, the behavior is dependent on the void ratio before compression. Specimen 15E-50 having the least void ratio shows the largest drained strength and the

least ultimate volumetric strain.

Mechanical consequences of suffusion are studied by comparing the drained monotonic compression test results of the suffusional specimens and the companion specimens without suffusion. [Muir Wood *et al.* \(2010\)](#) concluded that internal erosion (suffusion) would lower the soil strength. [Figures 24~26](#) plot the stress ~ strain curves together with the corresponding volumetric strain curves for the compression stage of the soil specimens under an effective confining pressure of 50kPa. Commonly, the deviator stress of the suffusional specimens is larger at the same small strain level (within 1%) comparing to that of the specimen without suffusion while that value becomes less at the same medium level (approximately 1% ~ 16%). In other words, the suffusional soil specimens show a larger initial stiffness at the small strain level, whereas the stiffness of suffusional specimen, conversely, becomes less than the specimen without suffusion when it comes to the medium strain level. For the specimens with the initial fines contents of 25% and 15%, the stress ~ strain curves of the suffusional soil and the soil without suffusion converge at the large strain level (larger than 16%). The volumetric strain curves appear to be initially contractive then followed by dilation. One exception is found at specimen 35E-50 whereby the specimens of both with and without suffusion show the contractive behavior for the whole shearing stage.

A hypothetical explanation for such inconsistent soil behavior is given at the grain level. In this study, the seepage water is the fresh water with amounts of fluidized fines. It is possible that the movement of fines is impeded due to the restriction of constriction size

and accumulated at the contact points among coarse grains. With the progress of suffusion, the coarse grains are reinforced at those spots where fines have accumulated (Fig. 27). Therefore, the suffusional soil specimens show the larger strength and stiffness at the small strain level (within 1%) with less volumetric deformation. However, the reinforcement may be deteriorated for the subsequent compression, which corresponding to the medium strain level (1%~16%) in this study. To validate this assumption and reveal the mechanical behavior of suffusional soil in detail, microscopic observations of specimens from different levels of shearing may be necessary.

Meanwhile, it is worth discussing the influence of end restraint. The end restraint refers to the phenomenon that the friction between the tested specimen and the end platens may greatly affect the dilation potential of soil at the end zone, causing an unreasonable decrease of pore pressure and increase of deviator stress. In this study, to ensure the successful drainage of fines, instead of a lubrication layer, a 0.005m-thick steel mesh with a smooth surface is used, which may influence the drained response of the suffusional specimens. It is considered as the deemed limitation for compression tests on suffusional soil.

6 Conclusions

The mechanisms of suffusion for saturated sand with different initial fines contents at isotropic stress states are presented in this paper. The binary mixtures consist of two types of silica sands (silica No.3 and No.8) with different dominant grain sizes. With larger

grain size, the silica No.3 works as the soil skeleton in the mixtures while the fine silica No.8 is the erodible fines. Suffusion tests are performed by the constant-flow-rate control in triaxial permeameter. The back pressure is applied to ensure the full saturation of tested soil. Cumulative eroded soil mass is continuously recorded by a consecutive monitoring system. The mechanical consequences of suffusion are assessed by conducting drained compression tests on suffusional soil specimens.

Hydraulic gradient dramatically drops with the progress of suffusion, indicated by the erosion of large amounts of fines. Correspondingly, hydraulic conductivity, derived from Darcy's law, keeps increasing at this stage. Afterwards, the soil grains would gradually reach a new equilibrium when the hydraulic gradient and cumulative eroded soil mass become constant. A moderate decrease of hydraulic conductivity is detected after a significantly long period of test time, which might be caused by the clogging of fines inside tested specimens. Erosion of fines would result in the increase of contractive volumetric strain. The post-suffusion grain size distribution analysis indicates that the fines loss is larger in the upper layer. The saturation degree drops after suffusion test with the B-value larger than 0.93.

Assigned the seepage flow with the same velocity, the specimens under the larger effective confining pressure show less increments in hydraulic conductivity within the test range. The percentage of cumulative fines loss and volumetric strain induced by suffusion is the least in the specimens under the effective confining pressure of 200kPa and the largest in the specimens under the effective confining pressure of 50kPa.

Comparing the suffusion test results of the specimens with 35%, 25% and 15% initial fines content, respectively, the largest change of hydraulic conductivity occurs in the specimen with 35% initial fines content. Fines loss is larger for the specimens with larger initial fines content and correspondingly, the suffusion induced volumetric strain is larger. The change of void ratio is closely dependent on the volumetric strain during suffusion. In this series of suffusion tests, the tested specimens show contractive behavior and the post-suffusion void ratio increases.

The deviator stress of the specimens with suffusion is larger at the same small strain level compared to that of the specimens without suffusion. When it comes to the same medium strain level, the specimens with suffusion, however, show less deviator stress. For the specimens with the initial fines contents of 25% and 15%, the stress ~ strain curves of the suffusional soil and the soil without suffusion converge at the large strain level. In terms of stiffness, the suffusional soil specimens show a larger initial stiffness at the same small strain level, whereas that value becomes less at the same medium strain level. The inconsistency of the eroded soil behavior is assumed to be related to the soil fabric resulting from suffusion. Thus, microscopic observation may be necessary to reveal the mechanism in detail.

ACKNOWLEDGEMENT

The first author acknowledges the Japanese Government (Monbukagakusho: MEXT)

scholarship support for conducting this research. This work was supported by JSPS KAKENHI Grant Numbers 23760440 and 25420498.

NOTATION

D'_x : Grain size for which x% mass passing is finer of the coarse fraction of a grading curve (mm);

d'_x : Grain size for which x% mass passing is finer of the fines fraction of a grading curve (mm);

D_x : Grain size for which x% mass passing is finer of the filter (mm);

d_x : Grain size for which x% mass passing is finer of the base soil (mm);

e_0 : Initial void ratio after saturation;

e_c : Void ratio of the suffusional specimen without volumetric deformation;

e : Post-suffusion void ratio;

ε_v : Suffusion induced volumetric strain (%);

FC : Initial fines content by mass (%);

ΔFC : Cumulative fines loss by mass (%);

k : Hydraulic conductivity (m/s);

p' : Mean effective stress (kPa);

q : Deviatoric stress (kPa);

Q : Inflow rate (m³/s);

v : Darcy velocity (m/s);

V_f : Volume of fines;

V_c : Volume of coarse grains;

ΔV_f : Volume of eroded fines;

ΔV : Intergranular re-arrangement induced volume change;

Λ : Ratio of the increments of void volume to that of solid volume due to particle removal

(McDougall *et al.*, 2004, 2013)

REFERENCES

ASTM D2487, Standard Practice for Classification of Soils for Engineering Purposes (Unified Soil Classification System), Annual Book of ASTM Standards, Vol.04.08,

ASTM International, West Conshohocken

ASTM D4767-11, Standard Test Method for Consolidated Undrained Triaxial Compression Test for Cohesive Soils, Annual Book of ASTM Standards,

Vol.04.08, ASTM International, West Conshohocken

ASTM D7181-11, Method for Consolidated Drained Triaxial Compression Test for Soils, Annual Book of ASTM Standards, Vol.04.09, ASTM International, West

Conshohocken

Bendahmane, F., Marot, D. and Alexis, A. (2008), Experimental parametric study of suffusion and backward erosion, Journal of Geotechnical and Geoenvironmental

Engineering, Vol.134, No.1, 57~67

Burenkova, V.V. (1993), Assessment of suffusion in non-cohesive and graded soils.

Filters in Geotechnical and Hydraulic Engineering, Brauns, Heibaum & Schuler,

Balkema, Rotterdam, 357~360

- Chang, C.S. and Meidani, M. (2012), Dominant grains network and behavior of sand-silt mixtures: stress ~ strain modeling, *Int. J. Numer. Anal. Meth. Geomech.*, DOI: 10.1002/nag.2152
- Chang, D.S. and Zhang, L.M. (2011), A stress-controlled erosion apparatus for studying internal erosion in soils, *Geotechnical Testing Journal*, Vol.34, No.6, 579~589
- Chang, D.S. and Zhang, L.M. (2012), Critical Hydraulic Gradients of Internal Erosion under Complex Stress States, *Journal of Geotechnical and Geoenvironmental Engineering*, 10.1061/(ASCE)GT.1943-5606.0000871
- Chang, D.S. and Zhang, L.M. (2013), Extended internal instability criteria for soils under seepage, *Soils and Foundations*, Vol.53, No.4, 569~583
- Chapuis, R.P. (1992), Similarity of internal stability criteria for granular soils, *Can. Geotech. J.* Vol.29, 711~713
- Crosta, G. and di Prisco, C. (1999), On slope instability induced by seepage erosion, *Can. Geotech. J.*, Vol.36, 1056~1073
- Evans, J.C. and Fang, H. Y. (1988), Triaxial permeability and strength testing of contaminated soils, *Advanced Triaxial Testing of Soil and Rock*, ASTM STP 977, Donaghe, R.T., Chaney, R.C. and Silver, M.L., Eds., American Society for Testing and Materials, Philadelphia, 387~404
- Fannin, R.J. and Moffat, R. (2006), Observations on internal stability of cohesionless soils, *Géotechnique*, Vol.56, No.7, 497~500
- Fell, R. and Fry, J.-J. (2013), State of the Art on the Likelihood of Internal Erosion of Dams and Levees by Means of Testing (Chapter 1), *Erosion in Geomechanics Applied to Dams and Levees*, Bonelli, S., Ed., Wiley/ISTE, 1~99

- Fry, J.-J. (2012), Introduction to the Process of Internal Erosion in Hydraulic Structures: Embankment Dams and Dikes (Chapter 1), Erosion of Geomaterials, Bonelli, S., Ed., Wiley/ISTE, 1~36
- Fujisawa, K., Murakami, A. and Nishimura, S. (2010), Numerical analysis of the erosion and the transport of fine particles within soils leading to the piping phenomenon, Soils and Foundations, Vol.50, No.4, 471~482
- Goldin, A.L. and Rummyantsev, O. A. (2009), On the history of development of the seepage and seepage strength of soils issue in Russia and at Vedeneev VNIIG, International Workshop on Internal Erosion in Dams and Foundations, St. Petersburg, Russia, April, 2009.
- Hicher, P.-Y. (2013), Modelling the impact of particle removal on granular material behaviour, Géotechnique, Vol.63, No.2, 118~128
- Huang, Y.T., Huang, A.B., Kuo, Y.C. and Tsai, M.D. (2004), A laboratory study on the undrained strength of silty sand from Central Western Taiwan, Soil Dynamics and Earthquake Engineering, Vol.24, 733~743
- Indraratna, B., Rout, A.K. and Khabbaz, H. (2007), Constriction-Based retention criterion for granular filter design, Journal of Geotechnical and Geoenvironmental Engineering, Vol.133, No.3, 266~276
- JGS 0524-2000, Method for Consolidated-Drained Triaxial Compression Test on Soils, Standards of Japanese Geotechnical Society for Laboratory Shear Test, Japanese Geotechnical Society, 23~27
- JGS 0525-2000, Method for K_0 Consolidated-Undrained Triaxial Compression Test on Soils with Pore Water Pressure Measurement, Standards of Japanese Geotechnical

- Society for Laboratory Shear Test, Japanese Geotechnical Society, 28~34
- Ke, L. and Takahashi, A. (2012), Strength reduction of cohesionless soil due to internal erosion induced by one-dimensional upward seepage flow, *Soils and Foundations*, Vol.52, No.4, 698~711
- Ke, L. and Takahashi, A. (2014), Triaxial erosion test for evaluation of mechanical consequences of internal erosion, *Geotechnical Testing Journal*, Vol.37, No.2, 347~364
- Kenney, T.C. and Lau, D. (1985), Internal stability of granular filters, *Can. Geotech. J.* Vol.22, 215~225
- Kenney, T.C. and Lau, D. (1986), Internal stability of granular filters: Reply, *Can. Geotech. J.* Vol.23, 255~258
- Kezdi, A. (1979), *Soil Physics: Selected Topics (Developments in Geotechnical Engineering)*, Elsevier Science Ltd.
- Kovacs, G. (1981), *Seepage hydraulics*, Elsevier Scientific Publishing Company, Amsterdam, Netherlands
- Ladd, R.S. (1978), Preparing test specimens using undercompaction, *Geotechnical Testing Journal*, Vol.1, No.1, 16~23
- Locke, M., Indraratna, B. and Adikari, G. (2001), Time-dependent particle transport through granular filters, *Journal of Geotechnical and Geoenvironmental Engineering*, Vol.127, No.6, 521~529
- Mao, C.X. (2005), Study on piping and filters: part 1 of piping, *Rock and Soil Mechanics*, Vol.26, No.2, 209-215 (in Chinese)
- Marot, D. and Benamar, A. (2012), Suffusion, Transport and Filtration of Fine Particles in

- Granular Soil (Chapter 2), Erosion of Geomaterials, Bonelli, S., Ed., Wiley/ISTE, 39~75
- McDougall, J. and Pyrah, I.C. (2004), Phase relations for decomposable soils, *Géotechnique*, Vol.54, No.7, 487~493
- McDougall, J., Kelly, D. and Barreto, D. (2013), Particle loss and volume change on dissolution: experimental results and analysis of particle size and amount effects, *Acta Geotechnica*, Vol. 8, 619~627
- Moffat, R.A. and Fannin, R.J. (2006), A large permeameter for study of internal stability in cohesionless soils, *Geotechnical Testing Journal*, Vol.29, No.4, 273~279
- Moffat, R., Fannin, R.J. and Garner, S.J. (2011), Spatial and temporal progression of internal erosion in cohesionless soil, *Can. Geotech. J.* Vol.48, 399~412
- Reboul, N., Vincens, E. and Cambou, B. (2010), A computational procedure to assess the distribution of constrictions sizes for an assembly of spheres, *Computers and Geotechnics*, Vol.37, 195~206
- Reddi, L.N., Lee, I. and Bonala, M.V.S. (2000), Comparison of internal and surface erosion using flow pump tests on a sand-kaolinite mixture, *Geotechnical Testing Journal*, Vol.23, No.1, 116~122
- Richards, K.S. and Reddy, K.R. (2007), Critical appraisal of piping phenomena in earth dams, *Bull Eng. Geo. Environ.*, Vol.66, 381~402
- Richards, K.S. and Reddy, K.R. (2012), Experimental investigation of initiation of backward erosion piping in soils, *Géotechnique*, Vol.62, No.10, 933~942
- Scholtès, L., Hicher, P.Y. and Sibille, L. (2010), Multiscale approaches to describe mechanical responses induced by particle removal in granular materials, *Comptes*

- Rendus Mecanique, 338, 627-638
- Shipton, B. and Coop, M.R. (2012), On the compression behaviour of reconstituted soils, Soils and Foundations, Vol.52, No.4, 668~681
- Silveira, A. (1965), An analysis of the problem of washing through in protective filters, Proceedings of 6th International Conference on Soil Mechanics and Foundation Engineering, Montreal, Canada, Vol.2, 551~555
- Skempton, A.W. and Brogan, J.M. (1994), Experiments on piping in sandy gravels, Géotechnique, Vol.44, No.3, 449~460
- Sterpi, D. (2003), Effects of the erosion and transport of fine particles due to seepage flow, International Journal of Geomechanics, Vol.3, No.1, 111~122
- Sugita, H., Sasaki, T. and Nakajima, S. (2008), Damage investigation of road embankment caused by the 2007 Noto Peninsula, Japan Earthquake, Public Works Research Institute Report
- Terzaghi, K. and Peck, R.B. (1948), Soil Mechanics in Engineering practice. 1st.Edition. John Wiley and Sons, New York
- Tomlinson, S.S. and Vaid, Y.P. (2000), Seepage forces and confining pressure effects on piping erosion, Can. Geotech. J. Vol.37, 1~13
- Uno, T. (2009), The state of the knowledge on seepage failure phenomena, Geotech. Eng. Mag., Vol.57, No.9, 1~5 (in Japanese)
- U.S. Army Corps of Engineers (1953), Filter experiments and design criteria. Technical Memorandum No. 3-360, Waterways Experiment Station, Vicksburg
- Vallejo, L.E. (2001), Interpretation of the limits in shear strength in binary granular mixtures, Can. Geotech. J. Vol.38, 1097~1104

- Vincens, E., Reboul, N. and Cambou, B. (2012), The Process of Filtration in Granular Materials (Chapter 3), Erosion of Geomaterials, Bonelli, S., Ed., Wiley/ISTE, 81~111
- Wan, C.F. and Fell, R. (2004), Investigation of rate of erosion of soils in embankment dams, Journal of Geotechnical and Geoenvironmental Engineering, Vol.130, No.4, 373~380
- Muir Wood, D. (2007), The magic of sands-The 20th Bjerrum Lecture presented in Oslo, 25 November 2005, Can. Geotech. J., Vol.44, 1329~1350
- Muir Wood, D., Maeda, K. and Nukudani, E. (2010), Modeling mechanical consequences of erosion, Géotechnique, Vol.60, No.6, 447-457
- Xiao, M. and Shwiyhat, N. (2012), Experiment investigation of the effects of suffusion on physical and geomechanic characteristics of sandy soils, Geotechnical Testing Journal, Vol.53, No.6, 1~11
- Yang, S.L., Sandven, R. and Grande, L. (2006), Steady-state lines of sand-silt mixtures, Can. Geotech. J., Vol.43, 1213~1219

Table 1 Physical properties of tested soil

Physical property	Silica No.3 (Coarse fraction)	Silica No.8 (Fines)	Specimen 35	Specimen 25	Specimen 15
Specific gravity, G_s	2.645	2.645	2.645	2.645	2.645
Fines content (%)	---	---	35	25	15
Maximum void ratio, e_{max}	0.94	1.33	0.74	0.77	0.79
Minimum void ratio, e_{min}	0.65	0.70	0.36	0.37	0.53
Median particle size D_{50} (mm) ⁽¹⁾	1.76	0.16	1.54	1.68	1.78
Effective particle size D_{10} (mm)	1.77	0.087	0.096	0.109	0.138
Uniformity coefficient C_u	1.5	1.7	18	17	13
Curvature coefficient C_c	1.1	0.96	0.25	7.9	7.9
$(H/F)_{min}$ ⁽²⁾	---	---	0.05	0.08	0.15
$(D_{15c}/d_{85f})_{gap}$ ⁽³⁾	---	---	7.9	7.9	7.9
Conditional factor of uniformity, h' ⁽⁴⁾	---	---	1.3	1.2	1.2
Conditional factor of uniformity, h'' ⁽⁵⁾	---	---	8.5	9.3	6.2
Grain Description	Sub-rounded ~ Sub-angular				

Note:

(1) D_x denotes the grain size finer than which the soil weight by percentage is $X\%$.

(2) F is the weight fraction of the soil finer than size d ; H is the weight fraction of the soil in the size ranging from d to $4d$.

(3) A soil could be split into the coarse fraction (c) and the fines fraction (f). D_{15c} is the grain size finer than which the soil weight by percentage is 15% for the coarse fraction; d_{85f} is the grain size finer than which the soil weight by percentage is 85% for the fines fraction.

(4) $h' = D_{90}/D_{60}$

(5) $h'' = D_{90}/D_{15}$

Table 2 Assessment of the mixture’s vulnerability to suffusion

Criteria	The mixture is internally stable if	Specimen 35	Specimen 25	Specimen 15
U.S. Army (1953)	$C_u < 20$	U ⁽¹⁾	U	S ⁽¹⁾
Istomina (1957) [Ref. Kovacs (1981)]	$C_u \leq 20$	U	U	S
Kezdi (1979)	$(D_{15c}/d_{85})_{\max} \leq 4$	U	U	U
Kenney and Lau (1985, 1986)	$(H/F)_{\min} \geq 1$ ($0 < F < 0.2$)	U	U	U
Burenkova (1993)	$0.76 \log(h'') + 1 < h' < 1.86 \log(h'') + 1$	U	U	U
Mao (2005)	$4P_f(1-n) \geq 1^{(2)}$	U	U	U

Note:

(1) “U” means Unstable; “S” means Stable;

(2) P_f is the fines content by weight in soil; n is the porosity, derived from Table 3.

Table 3 Details of test conditions

Specimen	Fines content before suffusion (%)	Initial void ratio	Post consolidation void ratio	Post suffusion void ratio	Mean effective stress (kPa)	Suffusion
35E-50	35	0.64	0.59	1.09	50	Y ⁽¹⁾
35E-100	35	0.60	0.55	0.92	100	Y
35E-200	35	0.59	0.55	0.80	200	Y
25E-50	25	0.61	0.57	0.81	50	Y
15E-50	15	0.68	0.68	0.78	50	Y
35N-50	35	0.60	0.56	---	50	N ⁽¹⁾
25N-50	25	0.61	0.58	---	50	N
15N-50	15	0.68	0.67	---	50	N
35E-50-R	35	0.62	0.60	1.00	50	Y
35E-100-R	35	0.60	0.56	0.95	100	Y
35E-200-R	35	0.64	0.57	0.77	200	Y

Note:

(1) “N” means no suffusion;

(2) “Y” means suffusion.

Table 4 Assigned Darcy velocity in suffusion tests

Specimen	Darcy velocity (m/s)
35E-50	0.00144
35E-100	0.00150
35E-200	0.00146
25E-50	0.00145
15E-50	0.00138

Table 5 Repeatability of suffusion tests

Specimen	Maximum hydraulic gradient	Post-suffusion hydraulic conductivity (m/s)	Percentage of cumulative fines loss (%)	Volumetric strain (%)
35E-50	11.7	0.028	25.0	3.9
35E-50-R	10.1	0.019	22.4	3.8
35E-100	5.68	0.008	22.7	3.2
35E-100-R	7.17	0.010	22.7	3.6
35E-200	10.5	0.008	13.9	2.8
35E-200-R	7.76	0.015	16.7	2.8

Constant-rate-flow test

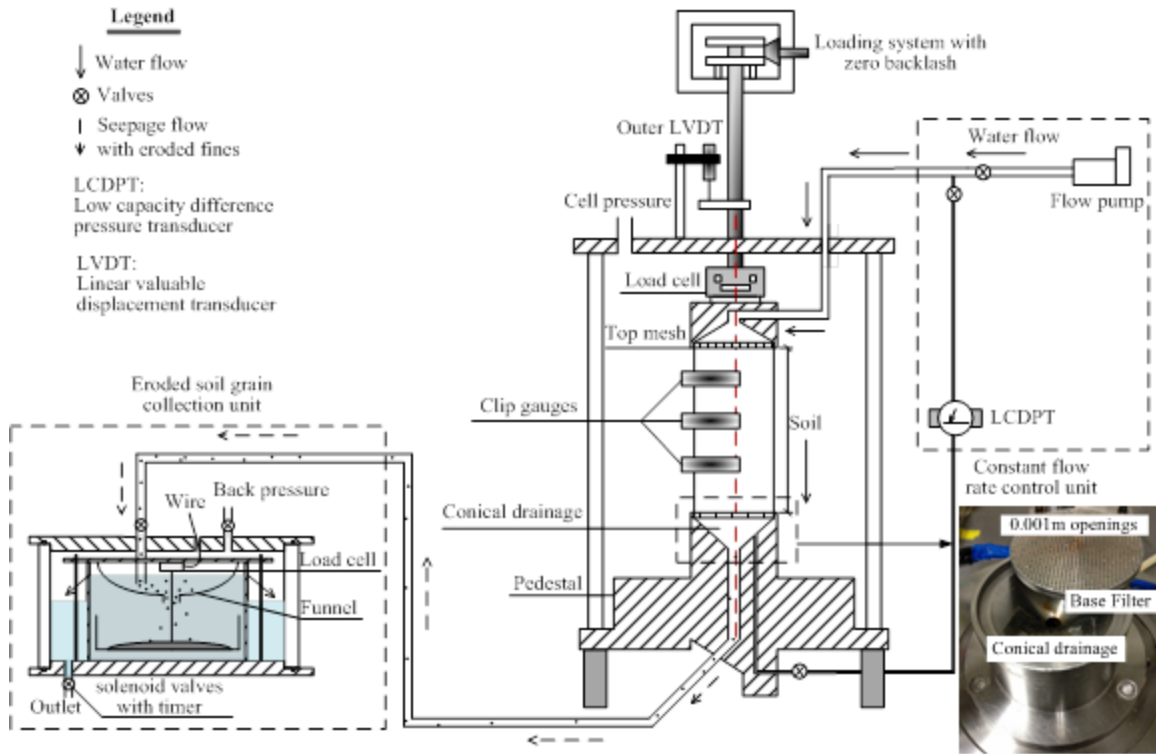


Fig.1 Schematic diagram of apparatus assembly



Fig.2 Photography of grains of silica No.3 (left) and No.8 (right)

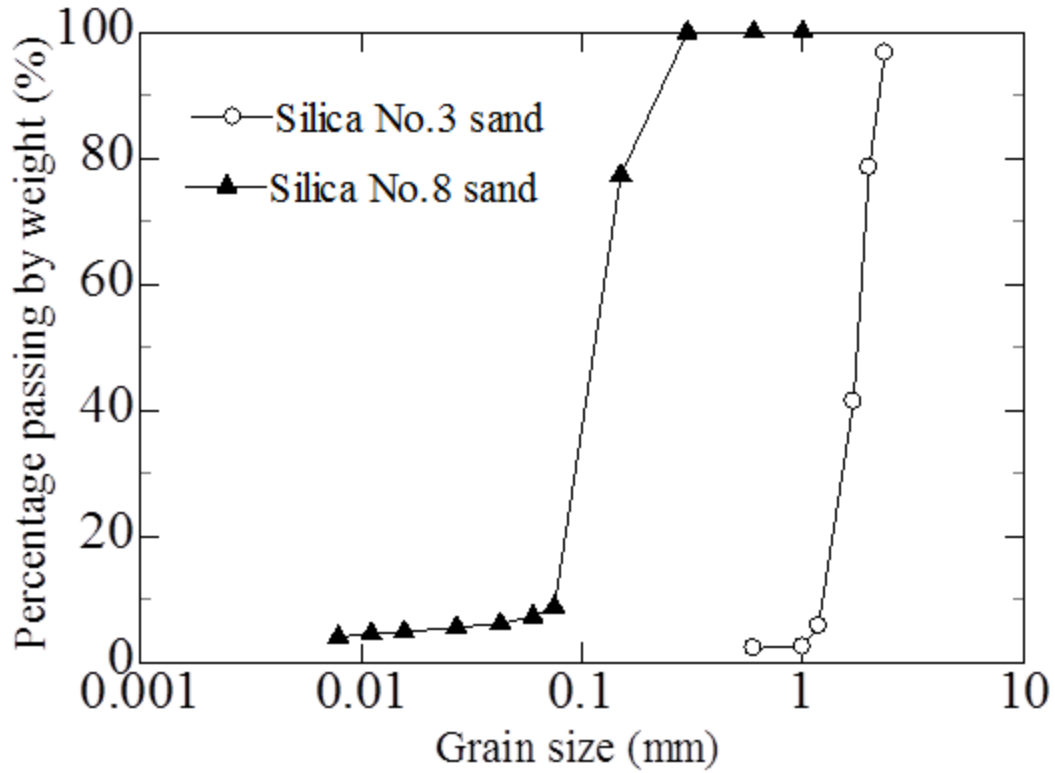


Fig.3 Grain size distribution curves of silica No.3 and No.8

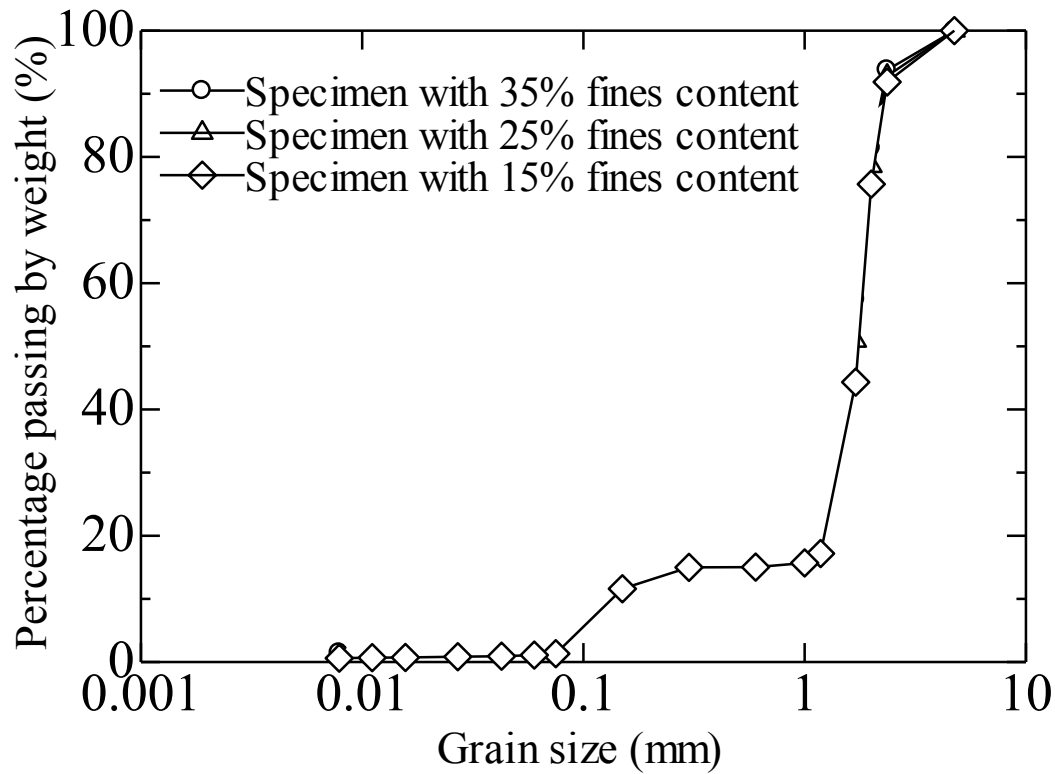


Fig.4 Grain size distribution curves of the mixtures

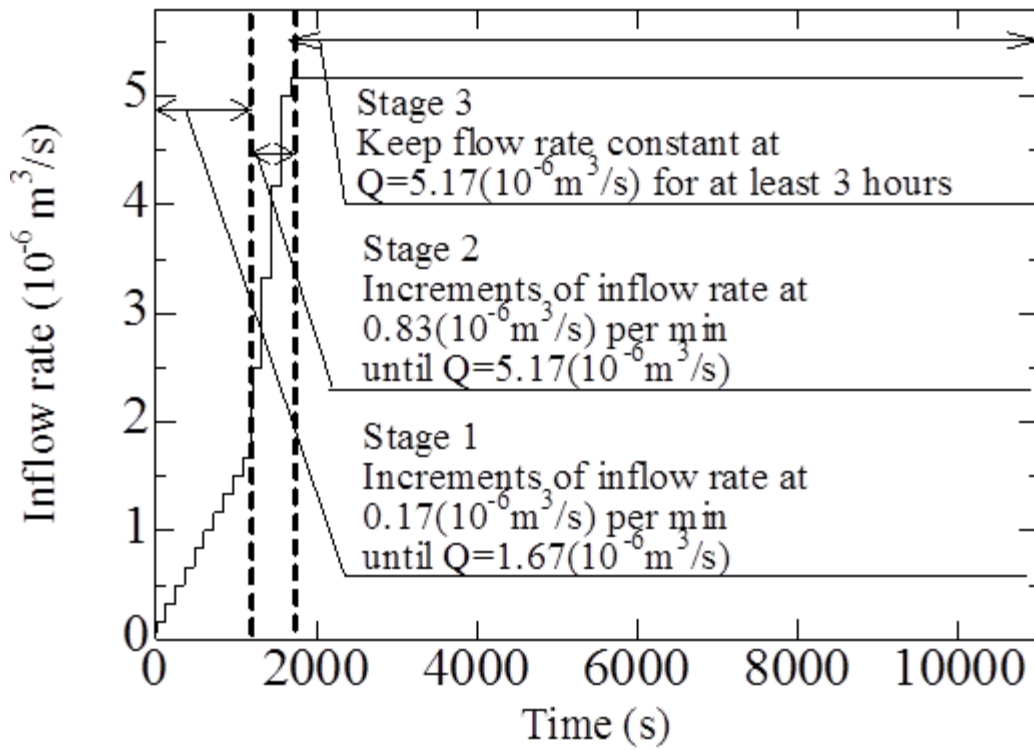


Fig.5 Inflow rate increments in seepage test

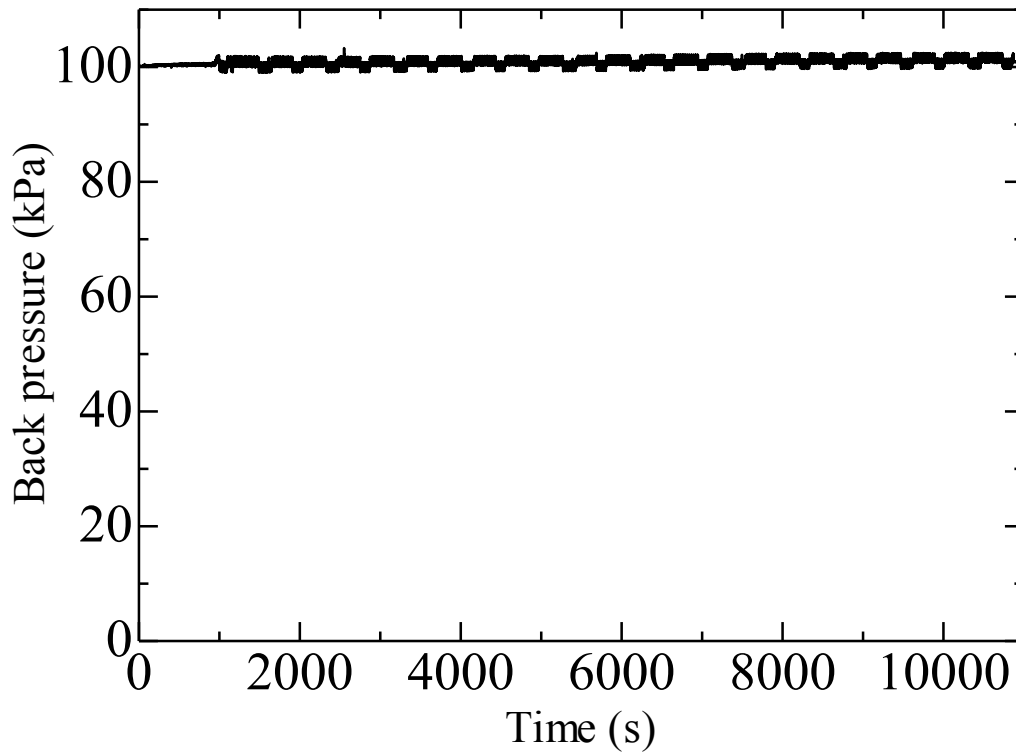
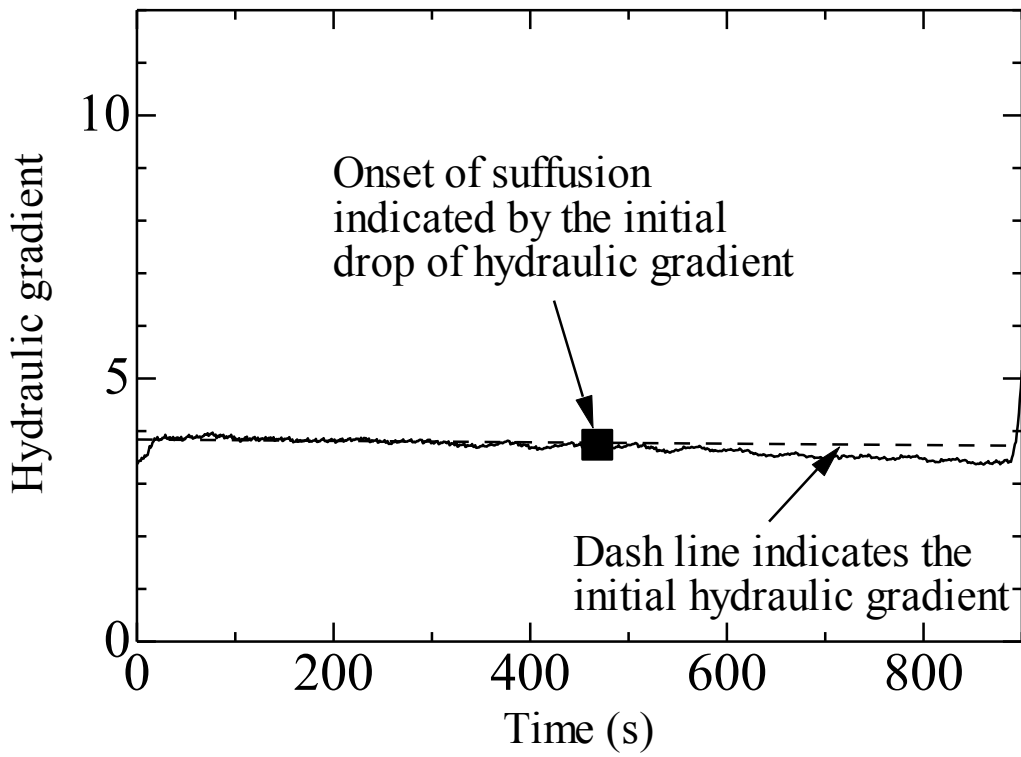
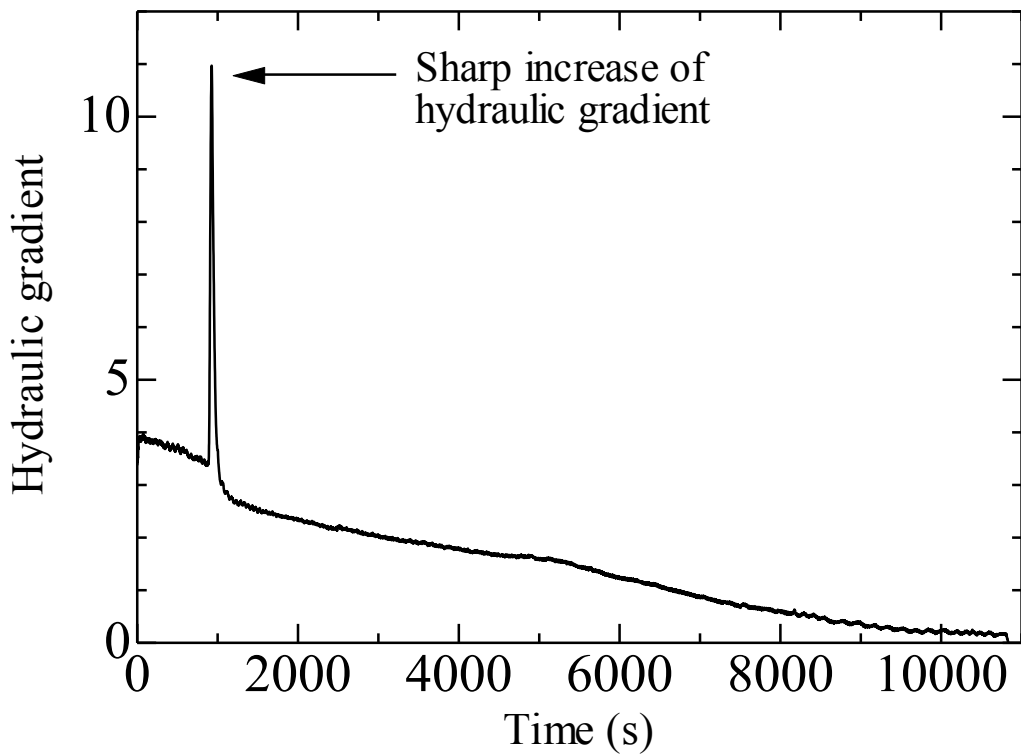


Fig.6 Maintained back pressure within seepage test period (specimen 35E-50)

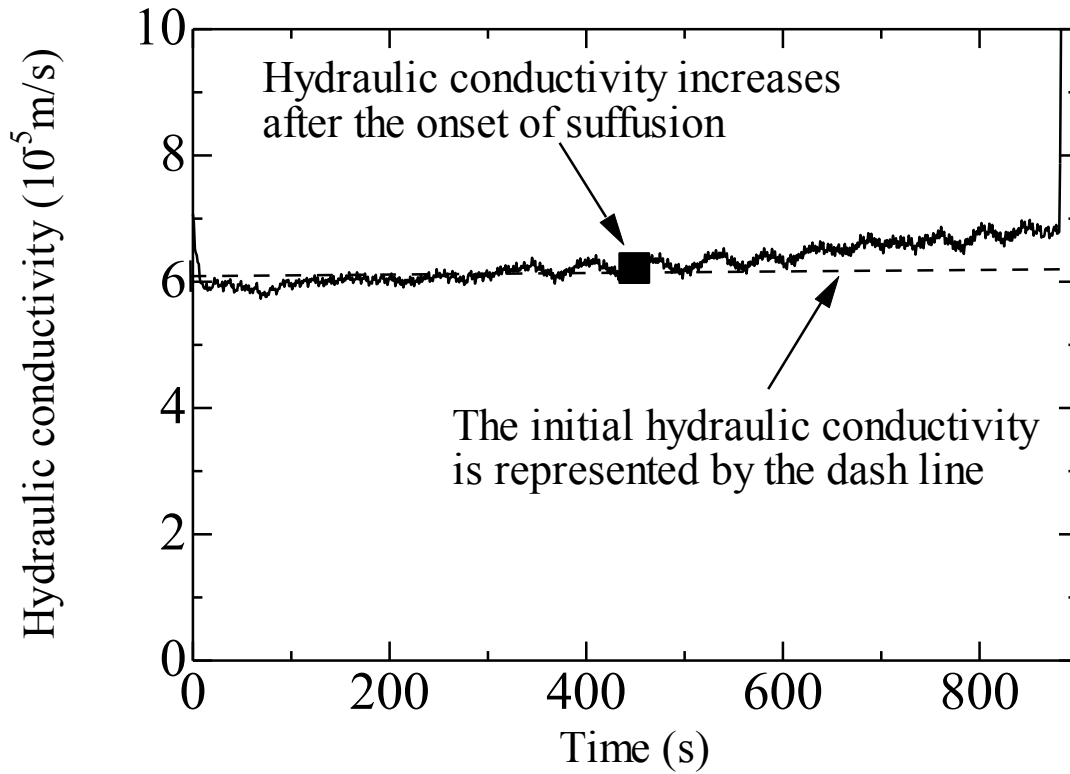


(a) 0s~900s of seepage test

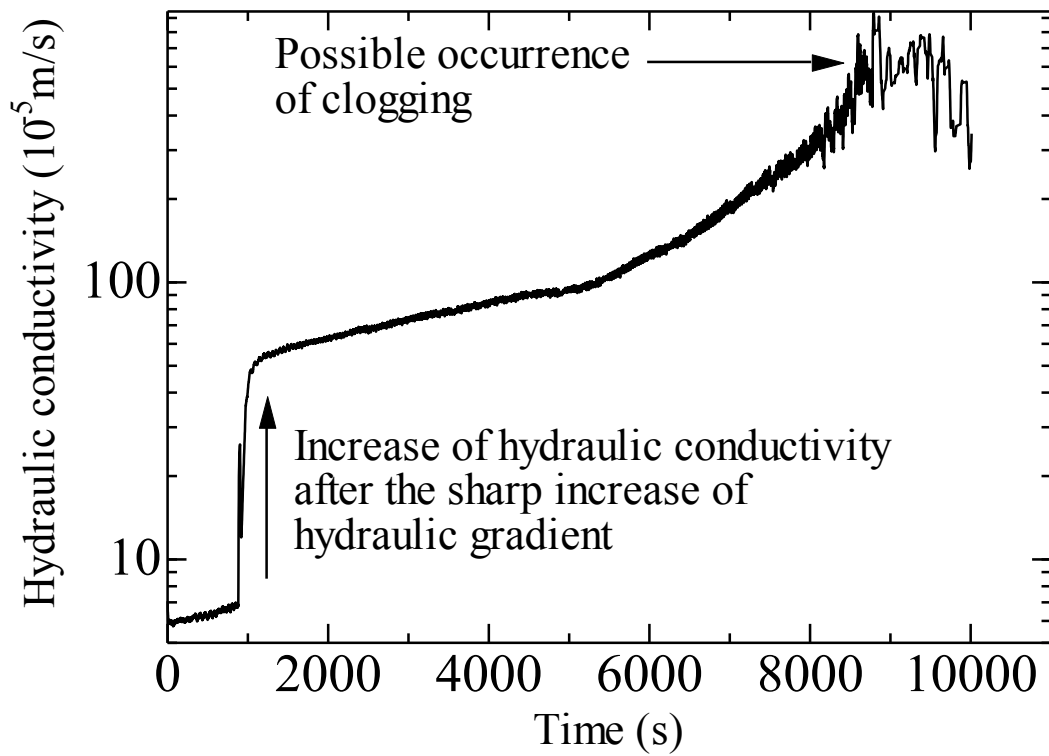


(b) Whole time period of seepage test

Fig.7 Hydraulic gradient within seepage test period (specimen 35E-50)



(a) 0s~900s of seepage test



(b) Whole time period of seepage test (semi-log scale)

Fig.8 Hydraulic conductivity within seepage test period (specimen 35E-50)

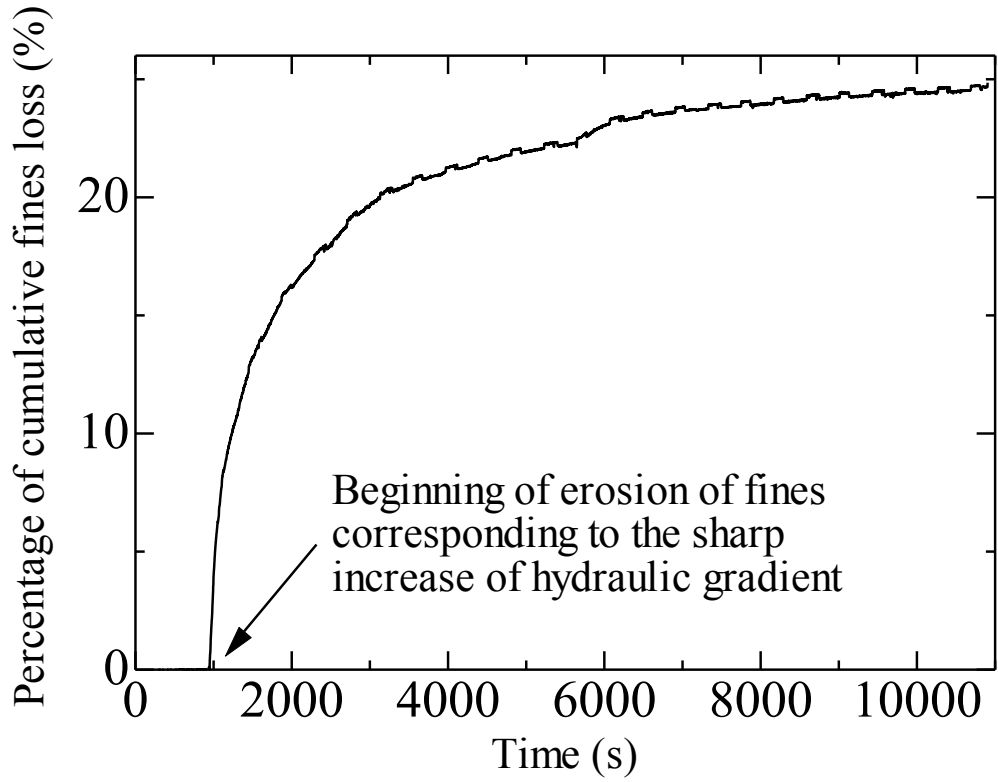


Fig.9 Percentage of cumulative fines loss within seepage test period (specimen 35E-50)

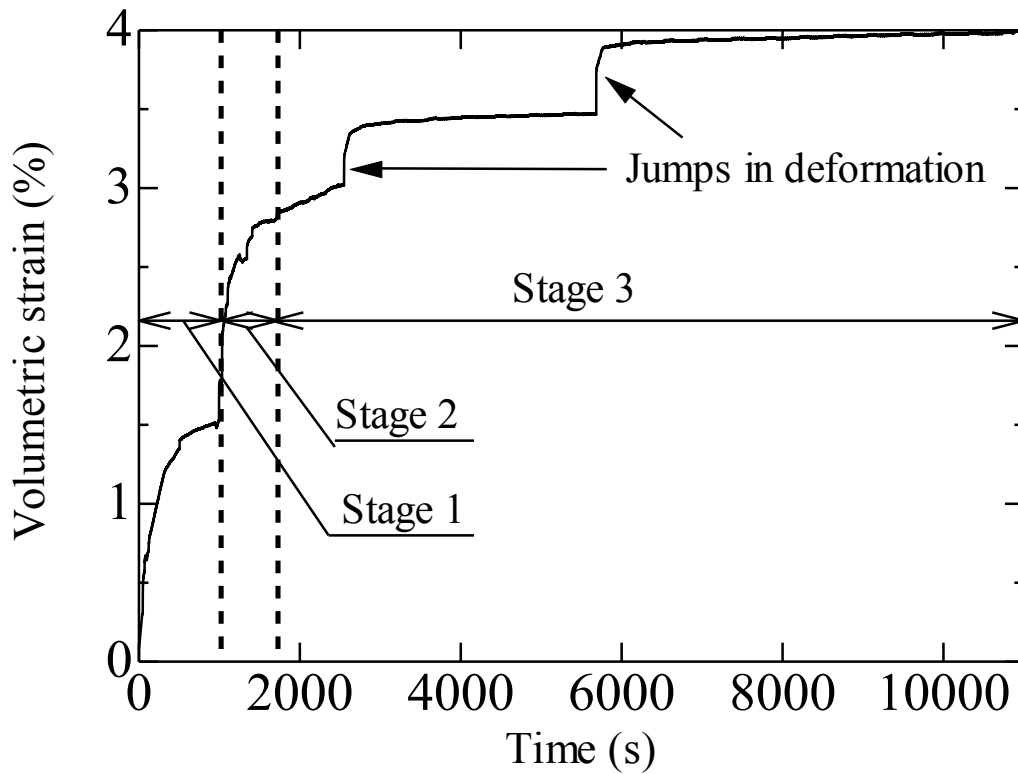


Fig.10 Volumetric strain within seepage test period (specimen 35E-50)

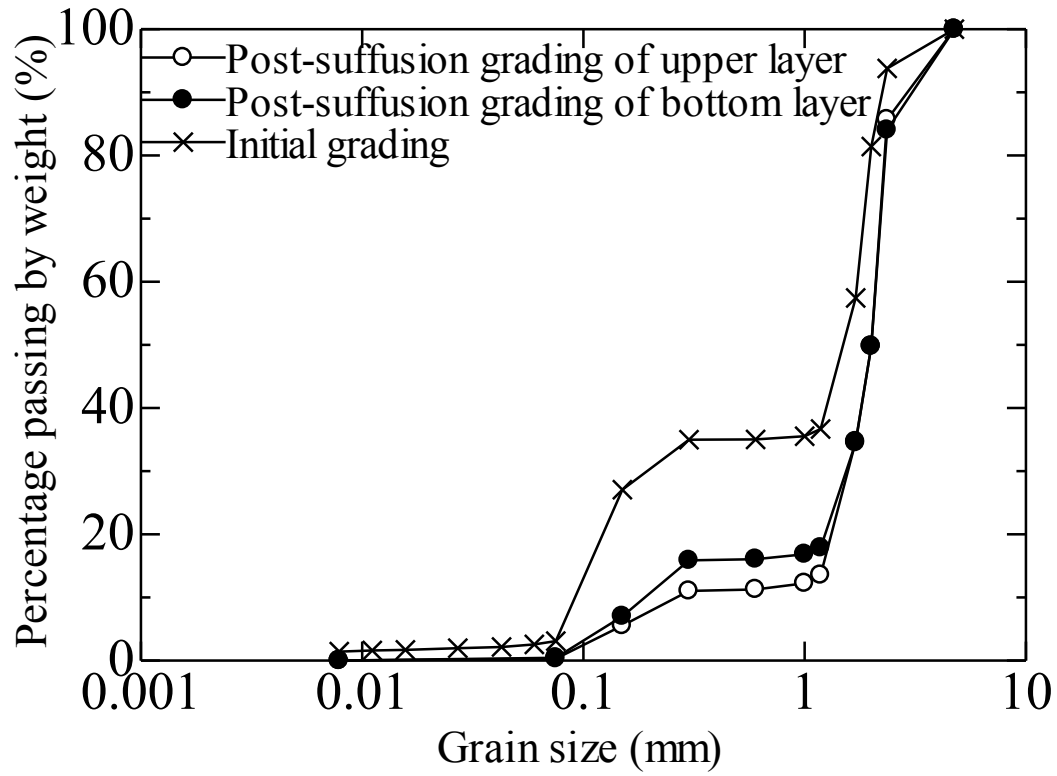


Fig.11 Grain size distribution curves of the post-suffusion specimen (specimen 35E-50)

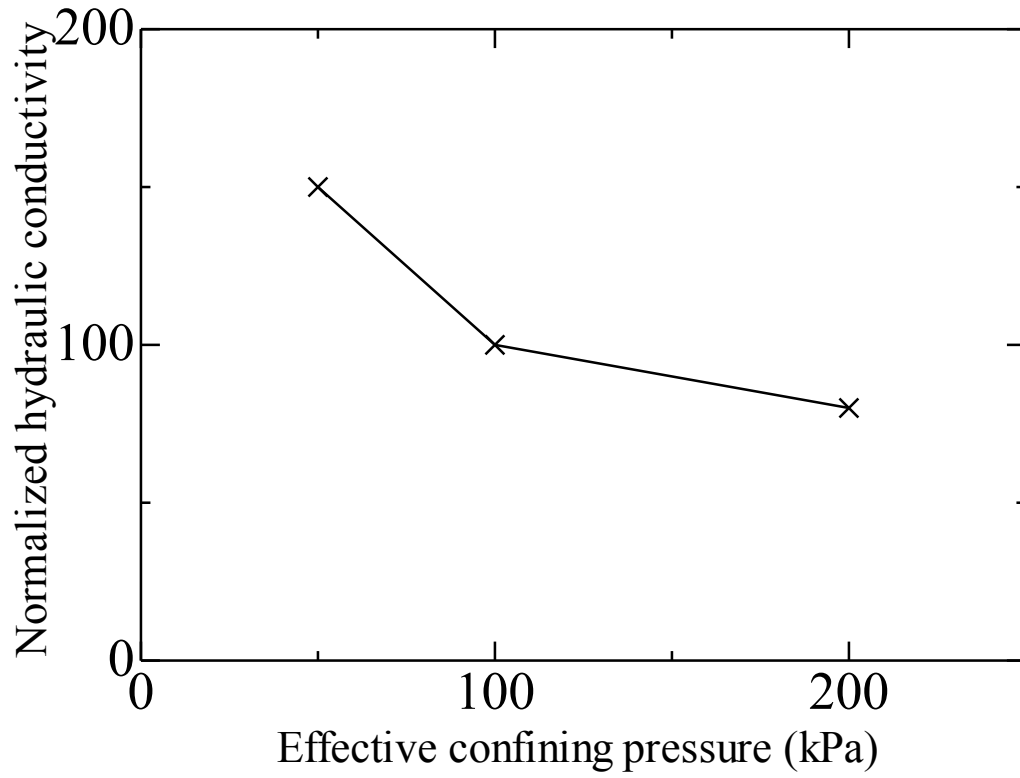


Fig.12 Normalized hydraulic conductivity versus effective confining pressure for specimens with 35% initial fines content

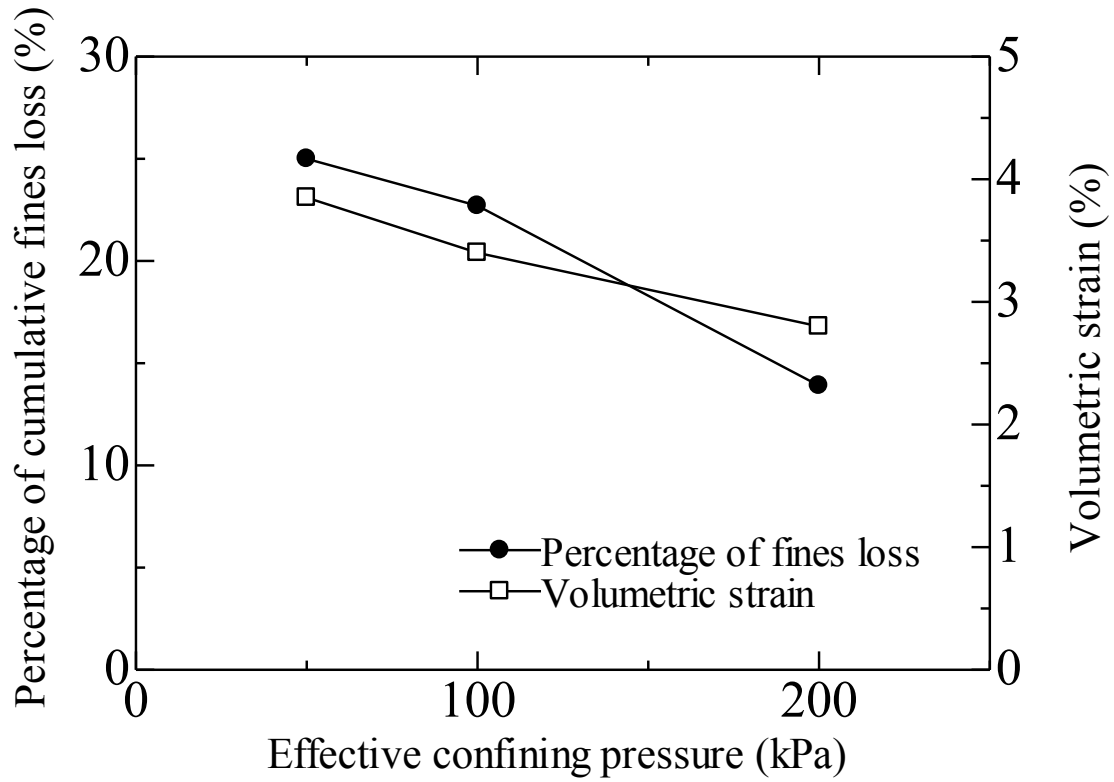
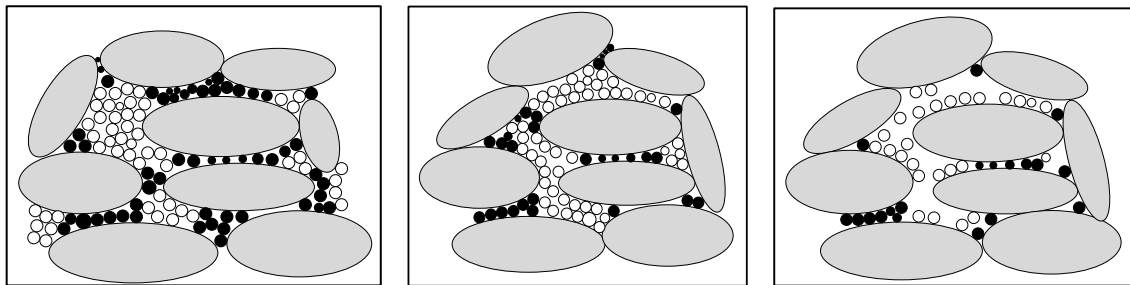


Fig.13 Percentage of cumulative fines loss and suffusion induced volumetric strain versus effective confining pressure for specimens with 35% initial fines content



(a) 35% initial fines content (b) 25% initial fines content (c) 15% initial fines content
 Fig.14 Schematic diagram of possible soil microstructure (the empty grains are erodible)

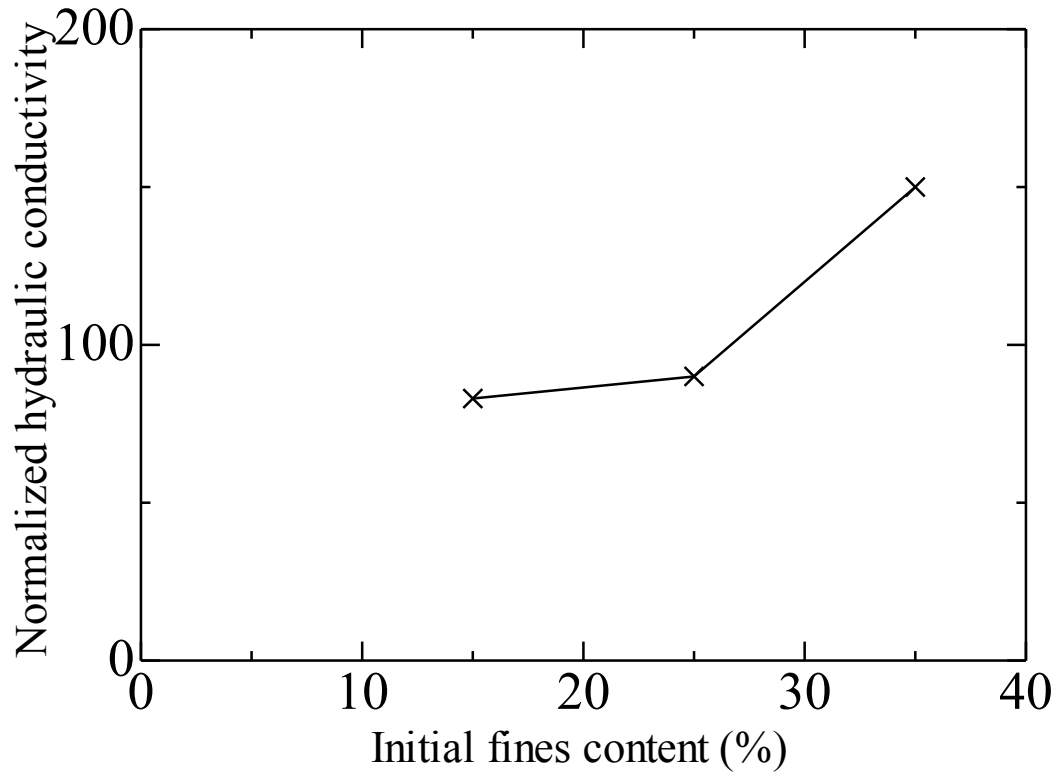


Fig.15 Normalized hydraulic conductivity versus initial fines content under an effective confining pressure of 50kPa

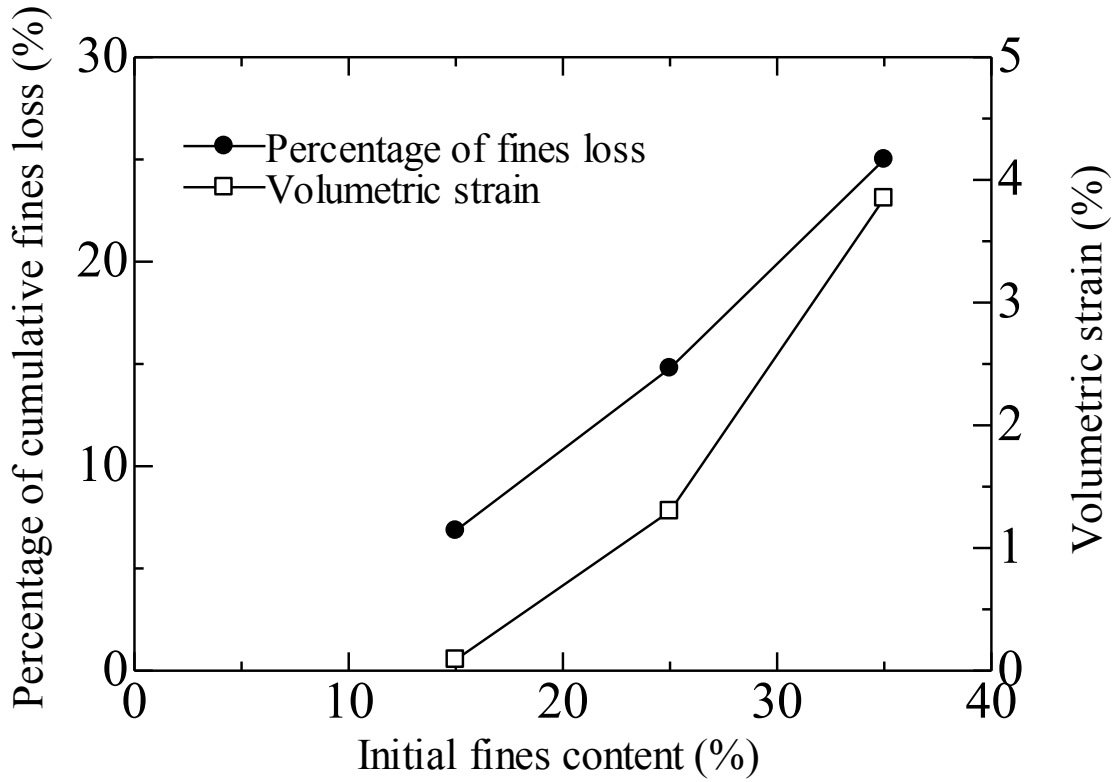


Fig. 16 Percentage of cumulative fines loss and suffusion induced volumetric strain versus initial fines content under an effective confining pressure of 50kPa

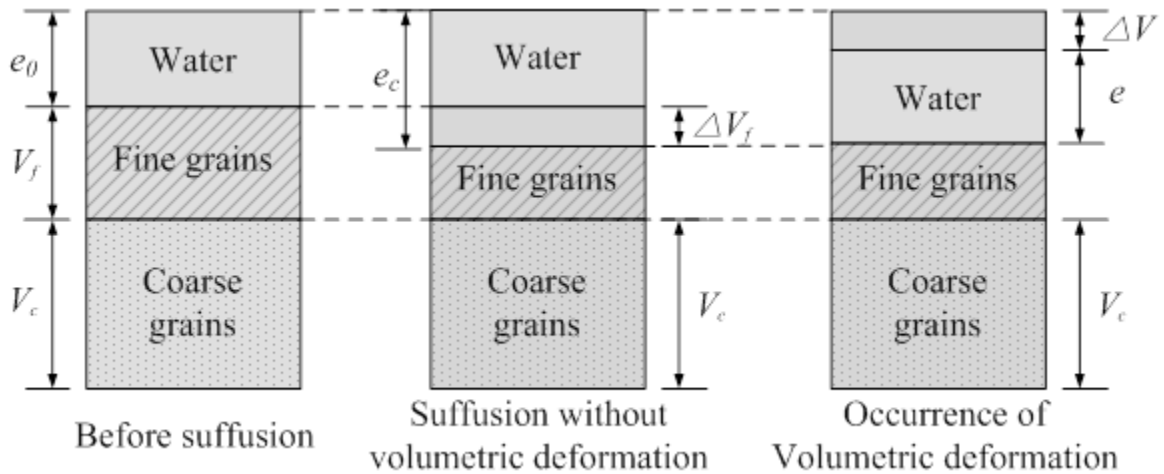
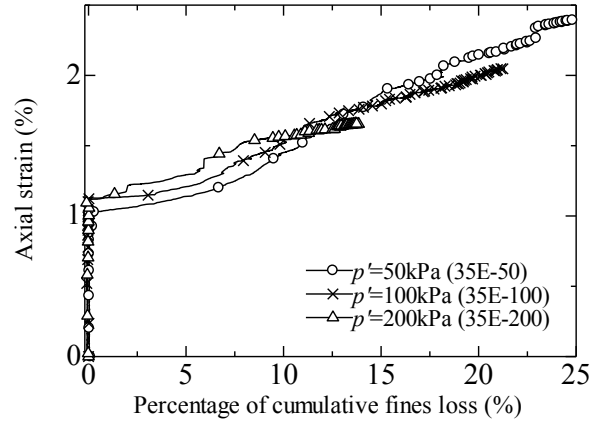
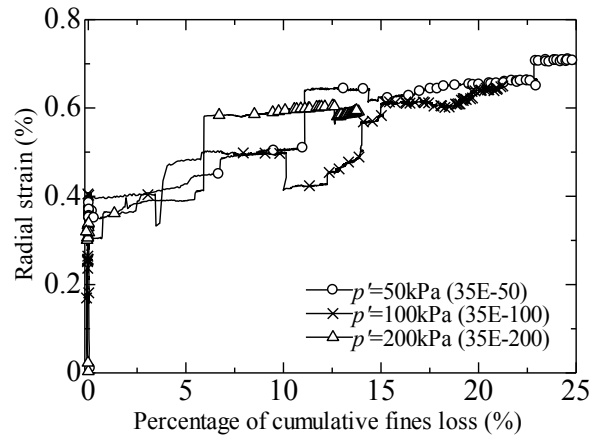


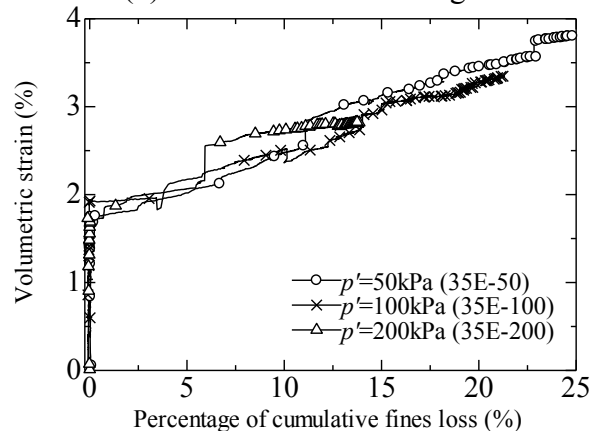
Fig. 17 Suffusion induced variation in soil phase relation



(a) Axial strain changes



(b) Radial strain changes



(c) Volumetric strain changes

Fig.18 Axial strain, radial strain and volumetric strain versus percentage of cumulative fines loss under different effective confining pressures for specimens with 35% initial fines content

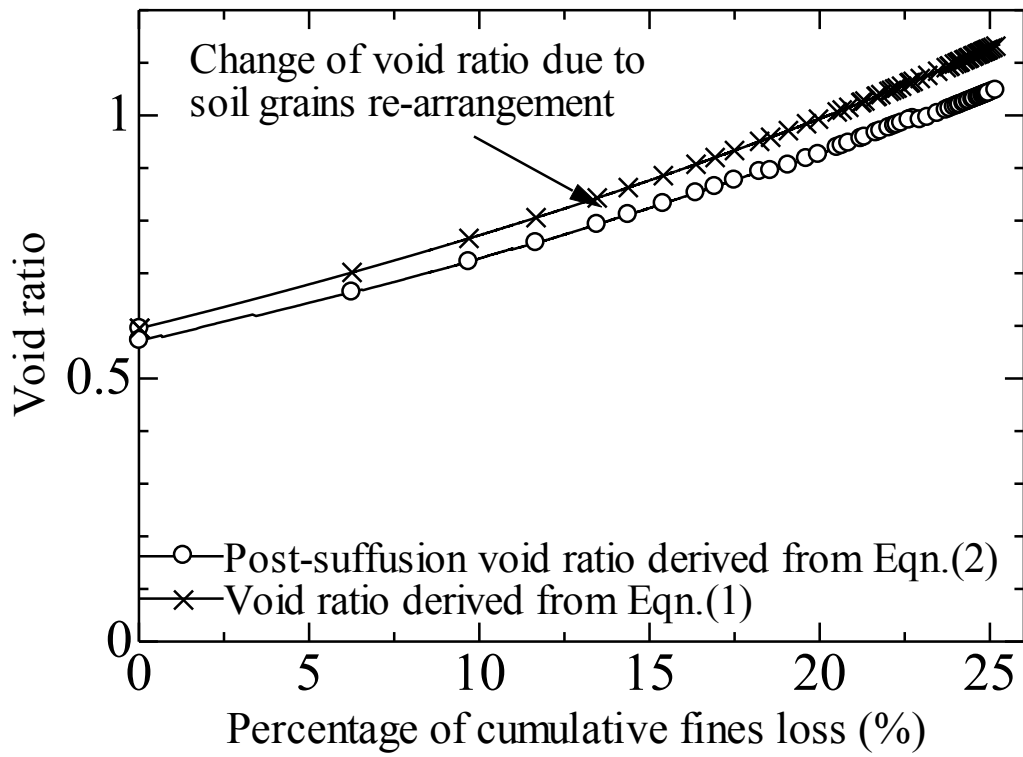
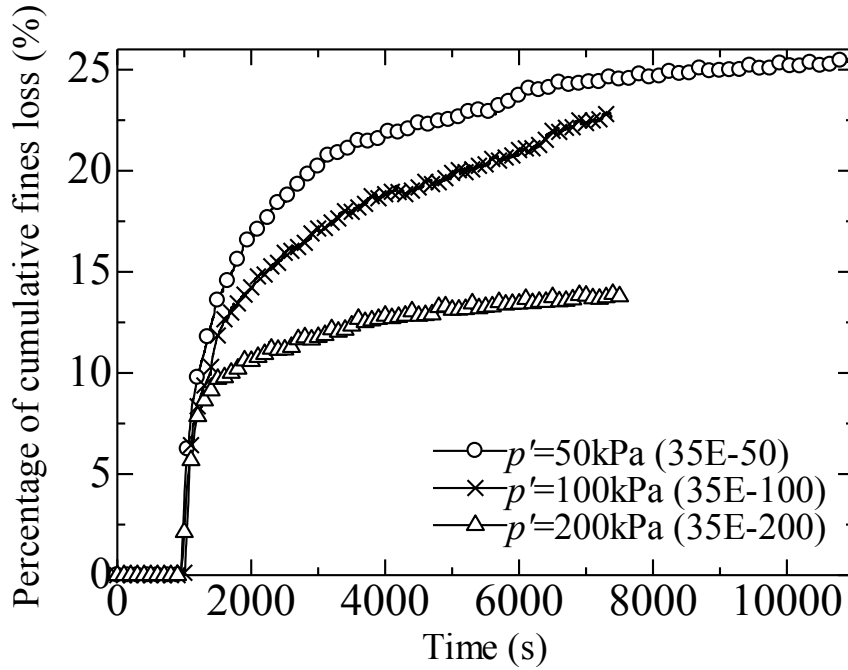
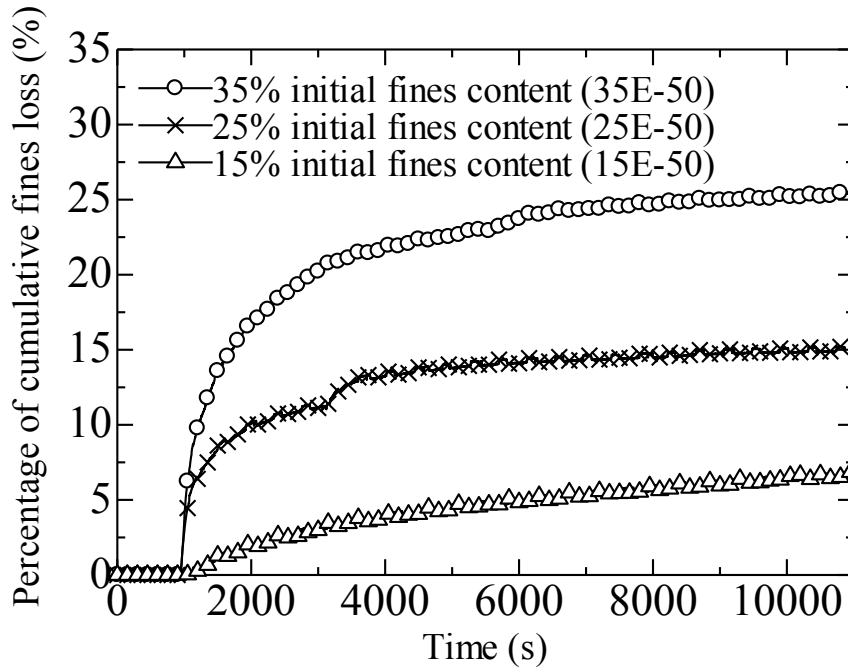


Fig.19 Void ratio versus percentage of cumulative fines loss under an effective confining pressure of 50kPa (specimen35E-50)

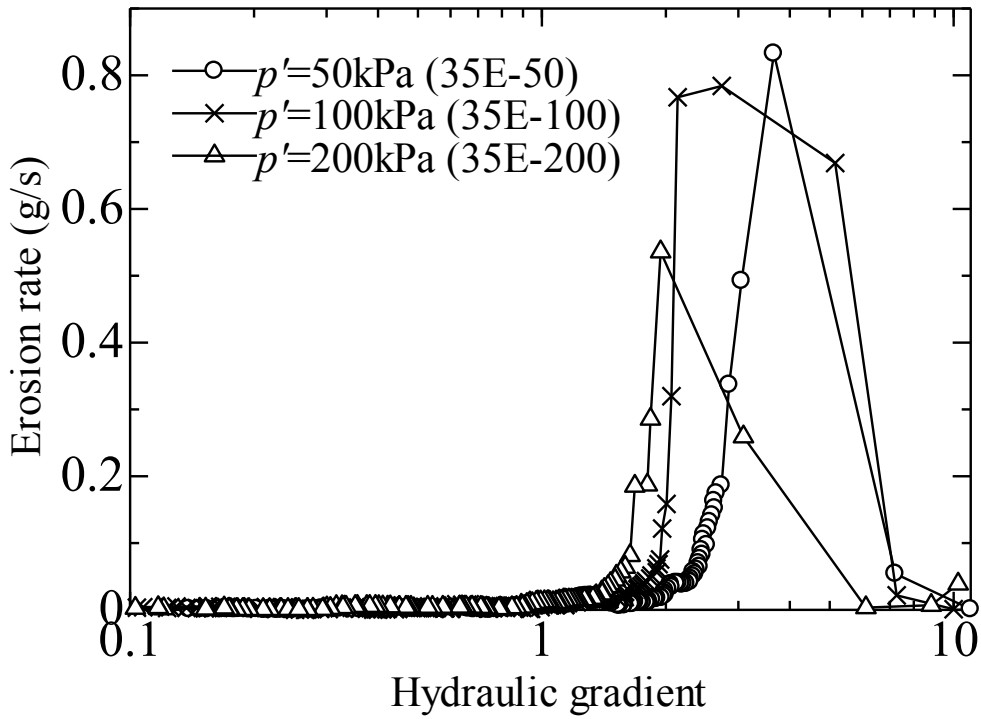


(a) Percentage of cumulative fines loss with time under different effective confining pressures for specimens with 35% initial fines content

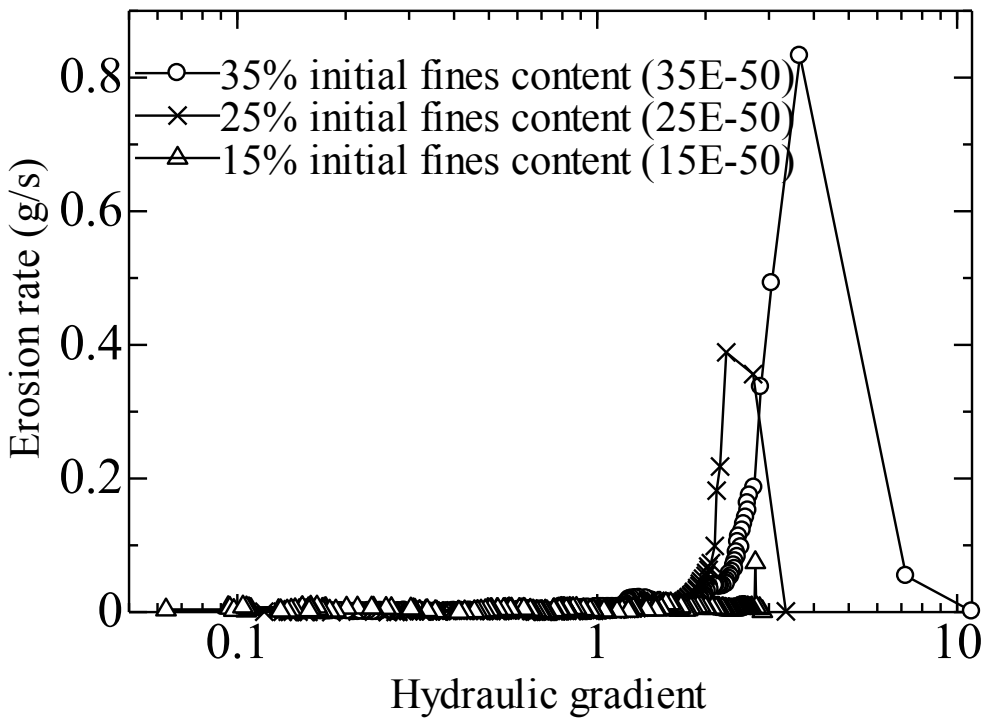


(b) Percentage of cumulative fines loss with time for specimens with different initial fines contents under an effective confining pressure of 50kPa

Fig.20 Percentage of cumulative fines loss within seepage test period

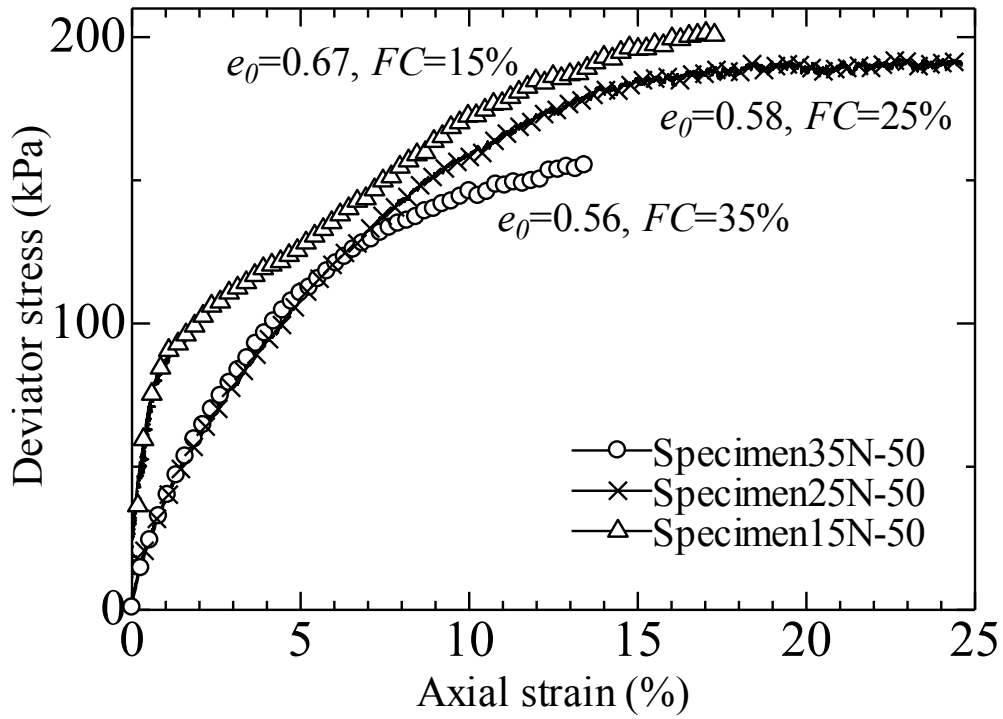


(a) Erosion rate with hydraulic gradient under different effective confining pressures for specimens with 35% initial fines content

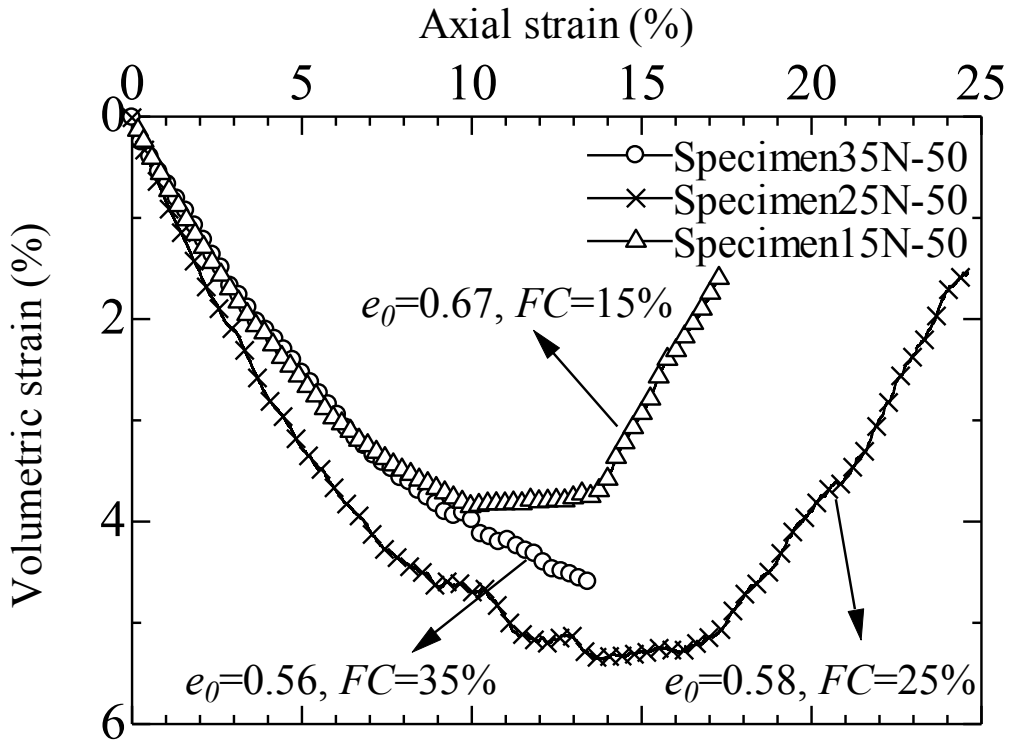


(b) Erosion rate with hydraulic gradient for specimens with different initial fines contents under an effective confining pressure of 50kPa

Fig.21 Evolution of erosion rate with hydraulic gradient (semi-log scale)

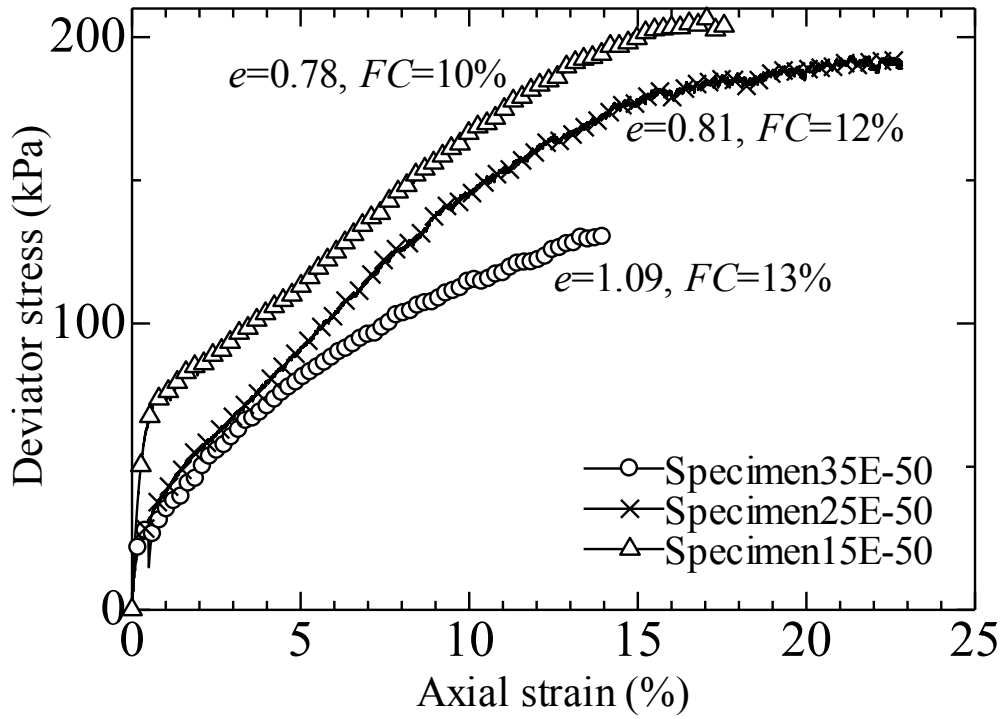


(a) Axial strain versus drained deviator stress

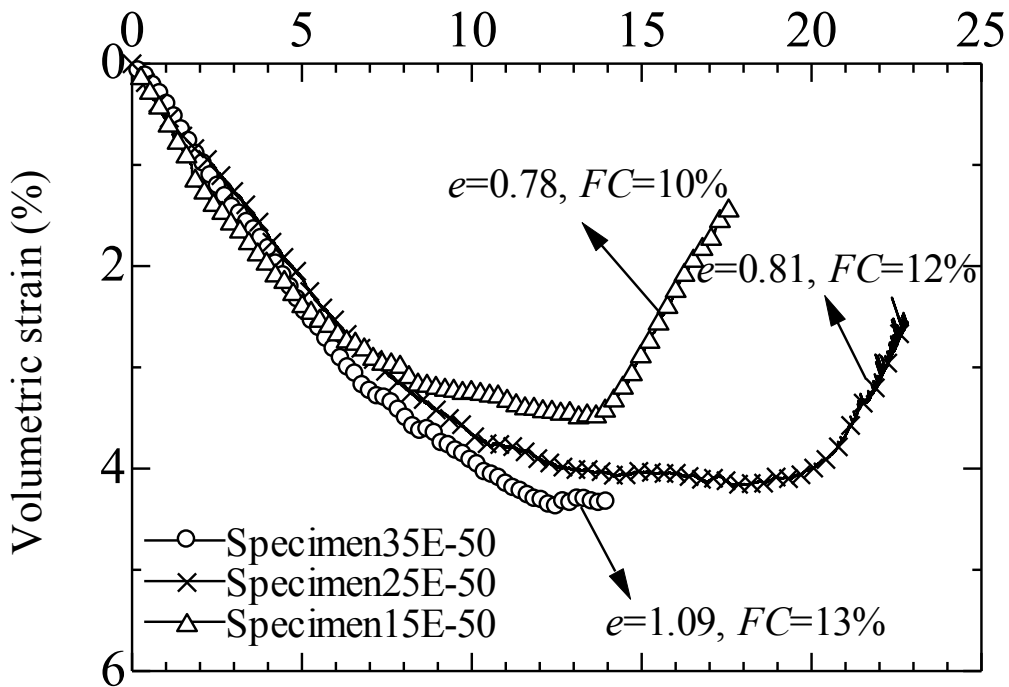


(b) Axial strain versus volumetric strain

Fig.22 Summary of drained response of the soil specimens without suffusion (35N-50, 25N-50 and 15N-50) under an effective confining pressure of 50kPa

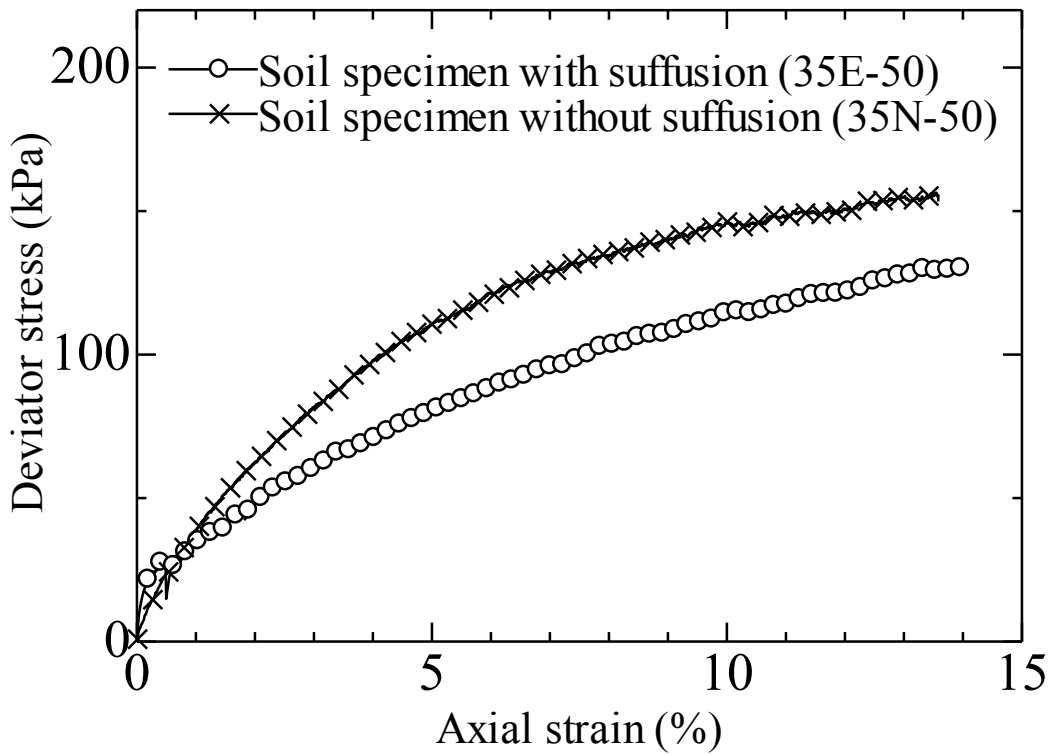


(a) Axial strain versus drained deviator stress

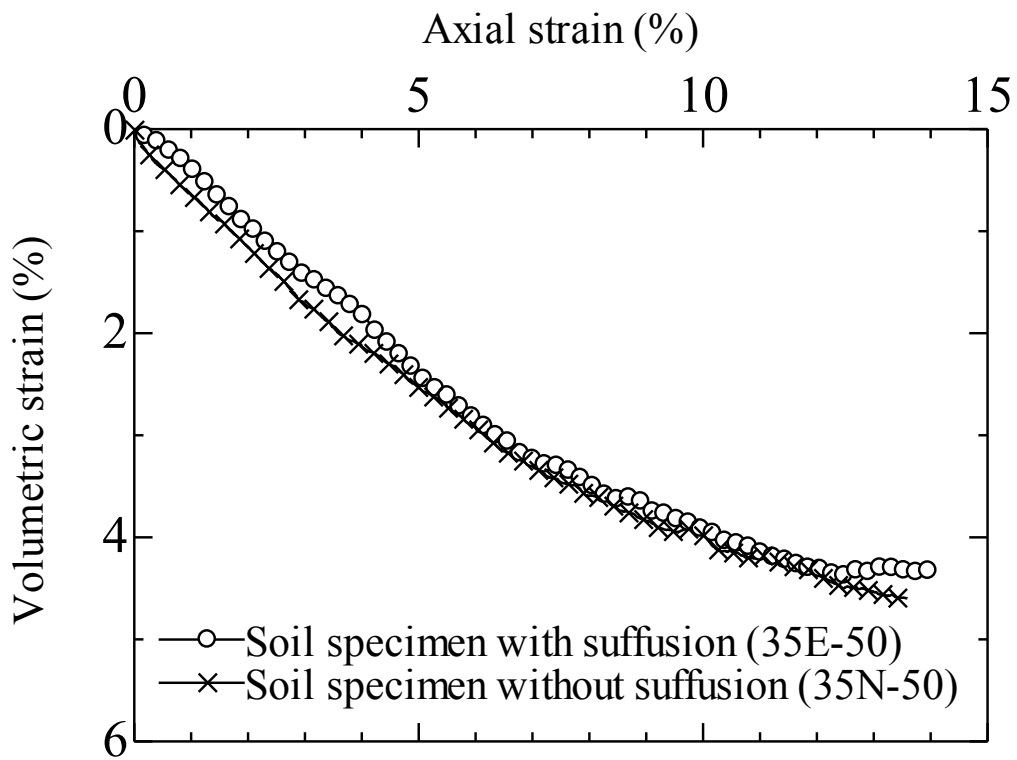


(b) Axial strain versus volumetric strain

Fig.23 Summary of drained response of the soil specimens with suffusion (35E-50, 25E-50 and 15E-50) under an effective confining pressure of 50kPa

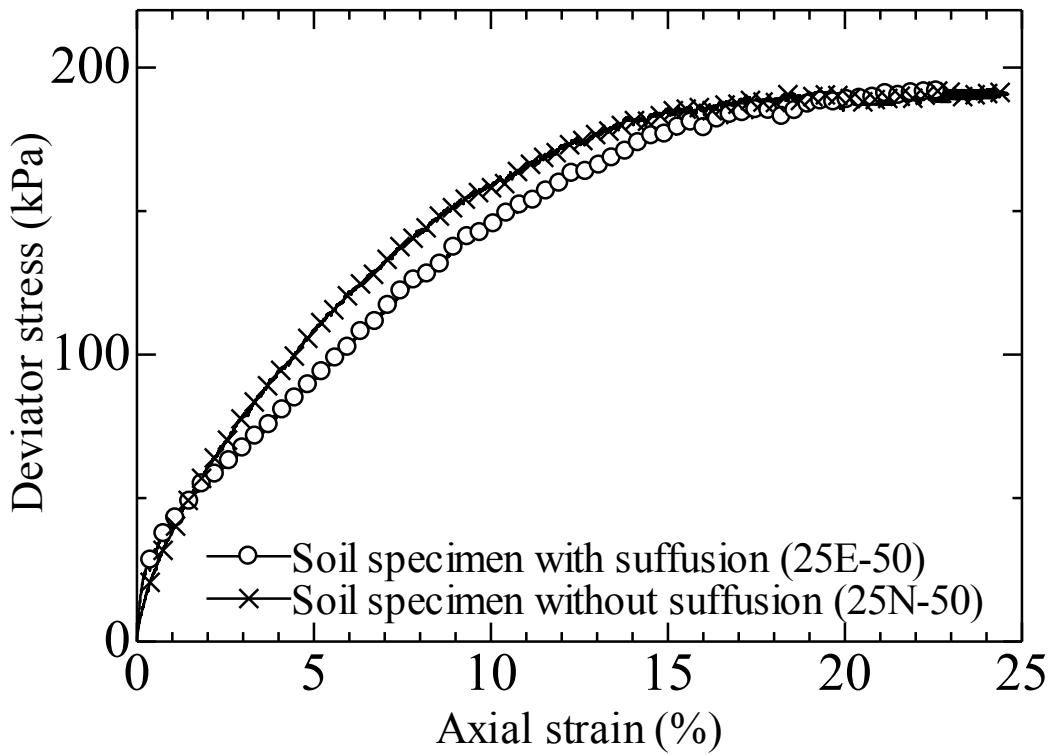


(a) Axial strain versus drained deviator stress

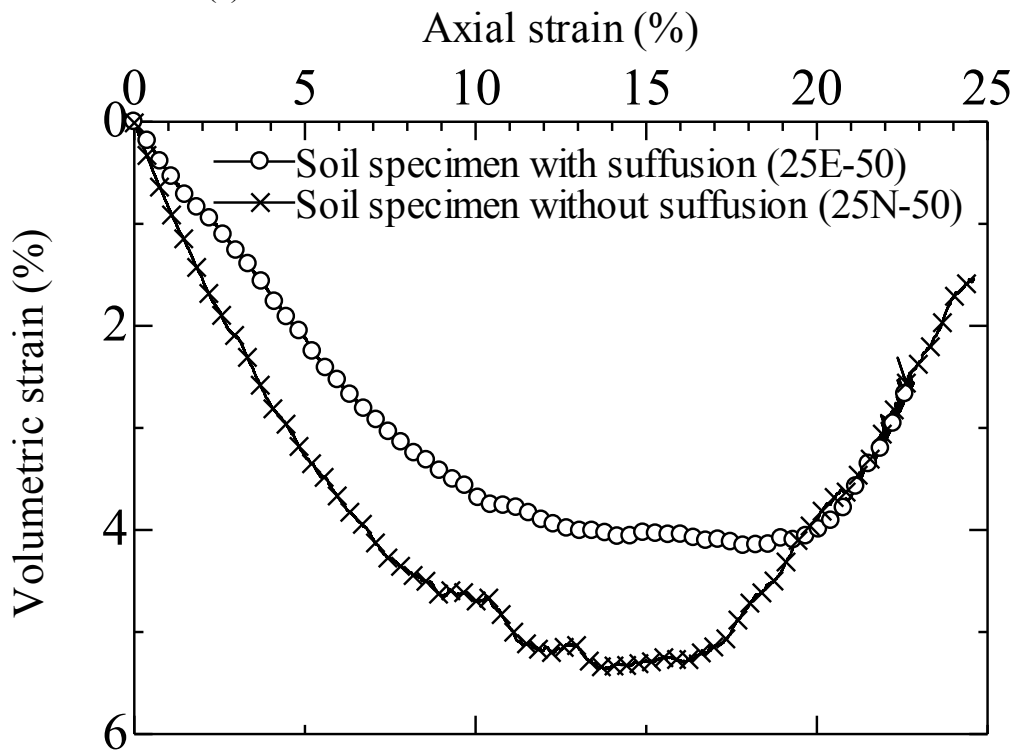


(b) Axial strain versus volumetric strain

Fig.24 Comparison of drained response of the soil specimen 35E-50 and 35N-50 under an effective confining pressure of 50kPa

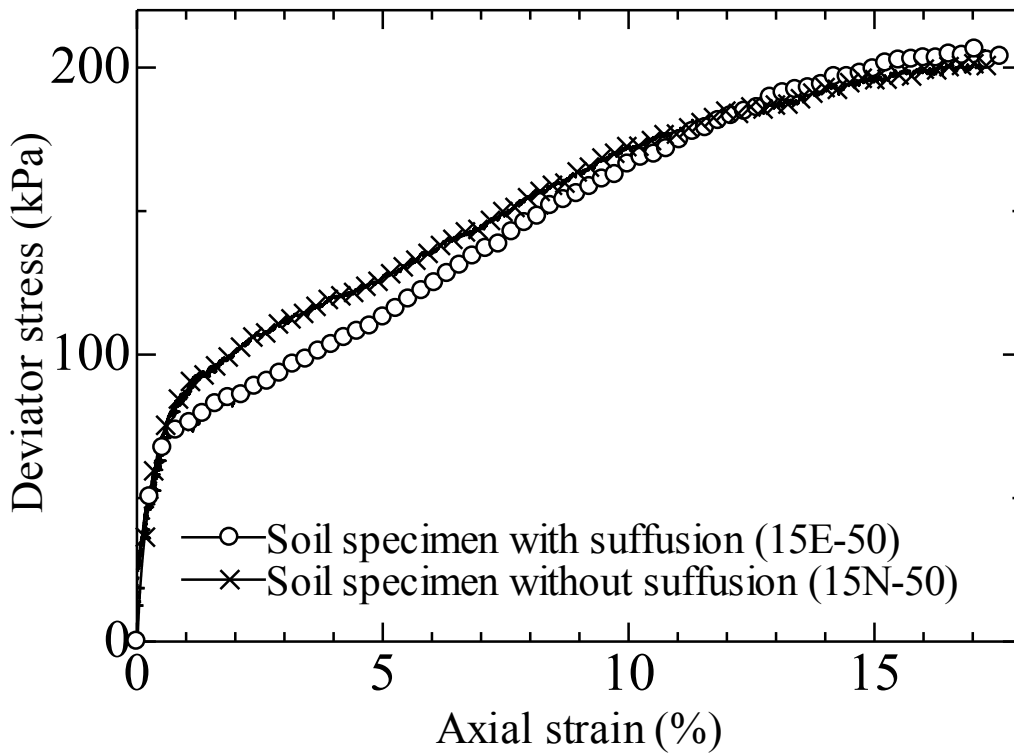


(a) Axial strain versus drained deviator stress

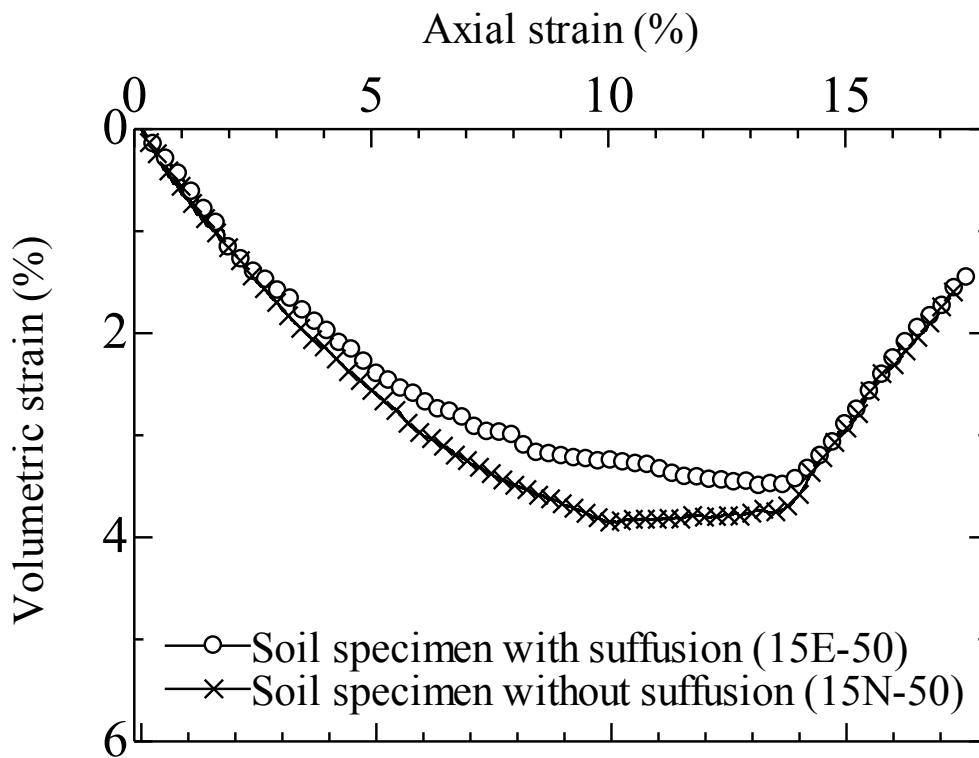


(b) Axial strain versus volumetric strain

Fig.25 Comparison of drained response of the soil specimen 25E-50 and 25N-50 under an effective confining pressure of 50kPa



(a) Axial strain versus drained deviator stress



(b) Axial strain versus volumetric strain

Fig.26 Comparison of drained response of the soil specimen 15E-50 and 15N-50 under an effective confining pressure of 50kPa

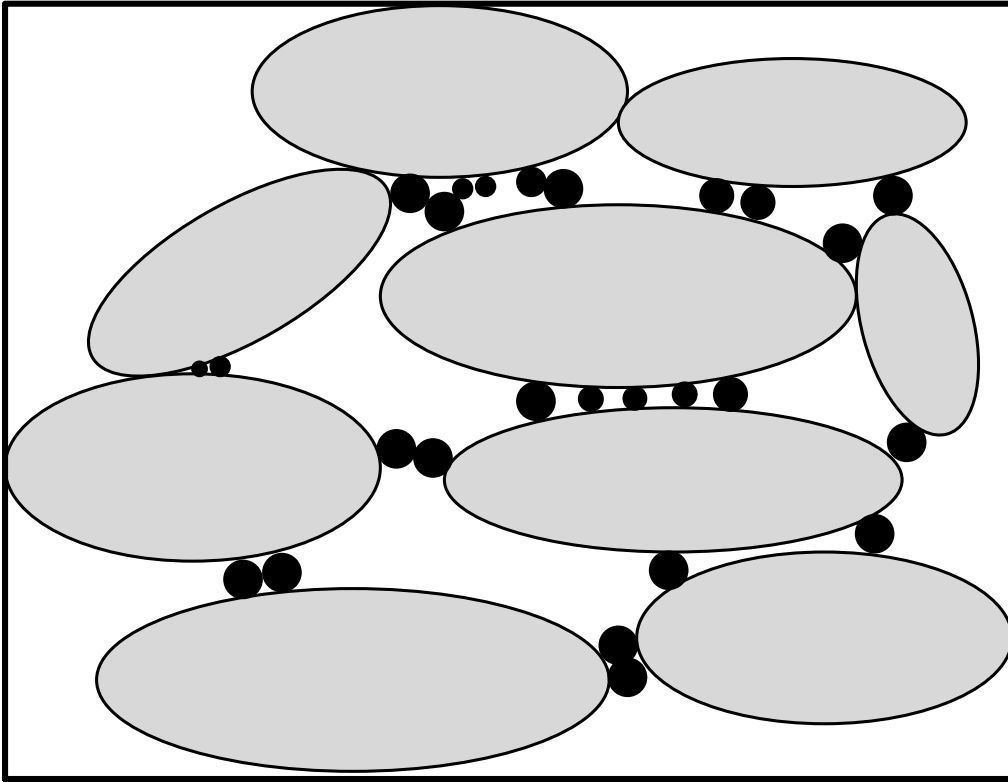


Fig.27 Possible post-suffusion soil microstructure with fines accumulated at the contact spots among coarse grains